Beta-Bond Scission and the Yields of H and CH_3 in the Decomposition of Isobutyl Radicals

Laura A. Mertens and Jeffrey A. Manion*

Chemical Sciences Division, National Institute of Standards and Technology, Gaithersburg, MD, 20899-8320

ABSTRACT: The relative rates of C-C and C-H β-scission reactions of isobutyl radicals (2-methylpropan-1-yl, C_4H_9) were investigated with shock tube experiments at temperatures of (950 to 1250) K and pressures of (200 to 400) kPa. We produced isobutyl radicals from the decomposition of dilute mixtures of isopentylbenzene and observed the stable decomposition products, propene and isobutene. These alkenes are characteristic of C-C and C-H bond scission, respectively. Propene was the main product, approximately 30 times more abundant than isobutene, indicating that C-C β-scission is the primary pathway. Uncertainty in the ratio of [isobutene]/[propene] from isobutyl decomposition is mainly due to a small amount of side chemistry, which we account for using a kinetics model based on JetSurF 2.0. Our data are well-described after adding chemistry specific to our system and adjusting some rate constants. We compare our data to other commonly used kinetics models: JetSurF 2.0, AramcoMech 2.0 and multiple models from Lawrence Livermore National Laboratory (LLNL). With the kinetics model, we have determined an upper limit of 3.0 % on the branching fraction for C-H β-scission in the isobutyl radical for the temperatures and pressures of our experiments. While this agrees with previous high quality experimental results, many combustion kinetics models assume C-H branching values above this upper limit, possibly leading to large systematic inaccuracies in model predictions. Some kinetics models additionally assume contributions from 1,2-H shift reactions – which for isobutyl would produce the same products as C-H β-scission – and our

upper limit includes possible involvement of such reactions. We suggest kinetics models should be updated to better reflect current experimental measurements.

1. INTRODUCTION

Alkyl radicals are ubiquitous in combustion chemistry.[1-3] They are typically formed from hydrocarbon decomposition or from radical attack on hydrocarbons and will readily decompose at high temperatures via β-scission (Scheme 1, R1b and R1a). While C-H bond scission preserves the original carbon chain and produces reactive H atoms, C-C bond scission breaks up the carbon chain and produces an alkyl radical. For example, in isobutyl (2-methylpropan-1-yl, C_4H_9) radicals (Scheme 1), C-H scission leads to isobutene (iC_4H_8) and H while C-C scission leads to propene (C_3H_6) and methyl (CH_3) radicals. Scissions of C-C bonds are favored over scission of C-H bonds, due mainly to the lower strength of the C-C bond.[1, 4] The competition between these reactions partially determines the intermediate alkenes and radicals in hydrocarbon combustion and pyrolysis; because H atoms are a source of chain branching in combustion systems, the balance can affect predictions of fuel properties.

Scheme 1. Decomposition of the isobutyl radical.

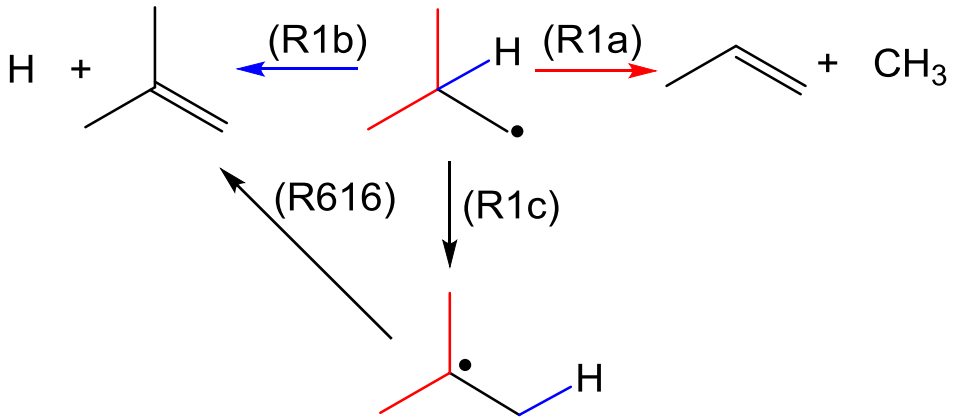

Since β-scissions are endothermic, their rate constants are often calculated from the reverse reactions – radical addition to an alkene[5-7] – and have additional uncertainties associated with the thermodynamics. While there have been some direct high quality measurements of

decomposition rate constants[7] and relative rate constants for C-H and C-C scission,[8-10] current combustion kinetics models use a large range of rate constants,[6, 11-15] most based on the reverse reactions.[6, 12, 15-19] There is continuing debate about the influence of 1,2 H-shift isomerizations in small alkyl radicals, as reflected by conflicting assumptions and rates constants between the above referenced combustion models (Note: an *x*,*y* H-shift refers to a shift in the radical center from the *x* position to the *y* position via a hydrogen transfer.[20]). In alkyl radicals such as *n*-propyl and isobutyl, a 1,2 H-shift isomerization followed by beta C-C scission leads to the same products as C-H scission in the initial radical. The isobutyl case is illustrated in Scheme 1 where both R1b and R1c lead to isobutene and H. While we will argue later that the 1,2 H shift in isobutyl is unimportant, it cannot be distinguished from direct C-H scission based on the end products. Studies in the literature of C-H bond scission[8, 21-23] and 1,2 H shifts[9-10, 24-28] have yielded conflicting results, and this literature will be briefly reviewed in the discussion section and compared to our results.[8-10, 21-28]

In previous work,[29-30] we have used kinetics models based on JetSurF 2.0 to understand the chemistry in our shock tube and have observed generally good agreement between the model and our experiments. However, comparison of the experimental yields of some products with predictions from JetSurF 2.0[6] suggests that the model rate constants for C-H β-scission are too large relative to competing C-C bond scission. For example, in recent work[29] on the reaction of H and CH_3 with *n*-butane, JetSurF 2.0 greatly overpredicted the amount of butene from *n*-butyl decomposition (JetSurF calculated the rate constants for *n*-butyl decomposition from the reverse reactions.

Table 1. Rate constants for unimolecular reactions of isobutyl (R1a, R1b and R1c) used in common combustion models. Parameters are for the equation $k = A \times T^n \times \exp(-E_a/RT)$. A is in units of mol, s, cm; E_a/R is in K.

Model	Reaction	Rate Constants and Troe Parameters as Stated in the Mechanism	Comments	$(k_{1b} + k_{1c})/k_{1a}$ at 1200 K and 101.3 kPa
JetSurF 2.0[6]	iC_4H_8+H (+M) ↔ iC_4H_9 (+M)	$k_\infty = 1.33 \times 10^{13} \times \exp(-1640.85 / T)$ $k_0 = 6.26 \times 10^{38} \times T^{-6.66} \times \exp(-3522.54 / T)$ A= 1.0, T_3 = 1000.0, T_1 = 1310.0, T_2 = 48 097.0	Same as JetSurF rate constant for C_3H_6 + H ↔ *n*-C_3H_7 from Tsang.[31]	21.6 %
	C_3H_6 + CH_3 (+M) ↔ iC_4H_9 (+M)	$k_\infty = 9.60 \times 10^{10} \times \exp(-4027.6 / T)$ $k_0 = 1.30 \times 10^{28} \times T^{-4.27} \times \exp(-1223.4/ T)$ A=0.565, T_3 = 60 000.0, T_1 = 534.2, T_2 = 3007.2		
AramcoMech 2.0[11-12]	iC_4H_9 (+M) ↔ C_3H_6 + CH_3 (+M)	k(0.1 atm) = $3.15 \times 10^{41} \times T^{-9.5} \times \exp(16\,850.8 / T)$ k(1.0atm) = $6.75 \times 10^{44} \times T^{-10.07} \times \exp(18\,724.3 /T)$ k(10.0 atm) = $7.79 \times 10^{44} \times T^{-9.7} \times \exp(20\,003.5 / T)$ k(100.0 atm) = $3.61 \times 10^{39} \times T^{-7.78} \times \exp(19\,919.0 / T)$	According to their code, "From K. Zhang estimated."	
	iC_4H_9 ↔ tC_4H_9	$k = 3.56 \times 10^{10} \times T^{0.88} \times \exp(17\,411.4 / T)$	From Matheu *et al.*[32]	
	iC_4H_8 + H (+M) ↔ iC_4H_9 (+M)	k(0.0013 atm) = $7.99 \times 10^{81} \times T^{-23.161} \times \exp(11\,191.1 / T)$ k(0.04 atm) = $4.24 \times 10^{68} \times T^{-18.427} \times \exp(9895.8 / T)$ k(1.0 atm) = $1.04 \times 10^{49} \times T^{-11.5} \times \exp(7728.9 / T)$ k(10.0 atm) = $6.2 \times 10^{41} \times T^{-8.892} \times \exp(7365.6 / T)$	From Miller and Klippenstein[33]	84.9 %
	iC_4H_8 + H (+M) ↔ iC_4H_9 (+M)	k(0.0013atm) = $1.85 \times 10^{26} \times T^{-5.83} \times \exp(1945.3 / T)$ k(0.04 atm) = $2.82 \times 10^{30} \times T^{-6.49} \times \exp(2753.0 / T)$ k(1.0 atm) = $3.78 \times 10^{28} \times T^{-5.57} \times \exp(3830.7 / T)$ k(10.0 atm) = $1.46 \times 10^{25} \times T^{-4.28} \times \exp(2640.8 / T)$ k(100.0 atm) = $4.22 \times 10^{27} \times T^{-4.39} \times \exp(9345.8 / T)$	From Miller and Klippenstein.[33] According to their code, they "refit to one parameter to avoid problems with negative k."	

LLNL Aromatics[15]	$iC_4H_9 \leftrightarrow tC_4H_9$	$k = 3.560 \times 10^{10} \times T^{0.880} \times \exp(17\,411.4 / T)$	From AramcoMech 1.3[19] which does not cite a reference for this rate constant, although it is identical to the rate constants from Matheu *et al*.[32]	3.4 %
	$iC_4H_8 + H \leftrightarrow iC_4H_9$	$k = 6.250 \times 10^{11} \times T^{0.510} \times \exp(1318.4 / T)$	From AramcoMech 1.3[19] who take the rate constant from Curran.[1]	
	$C_3H_6 + CH_3 \leftrightarrow iC_4H_9$	$k = 1.89 \times 10^{3} \times T^{2.670} \times \exp(3447.1 / T)$	From AramcoMech 1.3[19] who take the rate constant from Curran.[1]	
LLNL Isooctane[13]	$iC_4H_9 \leftrightarrow iC_4H_8 + H$	$k = 3.371 \times 10^{13} \times T^{0.124} \times \exp(16\,938.4 / T)$	Estimate decomposition rate constant as described by Curran *et al.*[18] in 1998: "because alkyl radical β-scission is endothermic, we now calculate the rate constant in the reverse, exothermic direction, i.e., the addition of an alkyl radical."	10.3 %
	$iC_4H_9 \leftrightarrow C_3H_6 + CH_3$	$k = 9.504 \times 10^{11} \times T^{0.773} \times \exp(15\,448.8 / T)$		
LLNL Biodiesel[14]	$iC_4H_9 \leftrightarrow iC_4H_8 + H$	$k = 4.980 \times 10^{32} \times T^{-6.23} \times \exp(20\,164.0 / T)$		6.8 %
	$iC_4H_9 \leftrightarrow C_3H_6 + CH_3$	$k = 1.640 \times 10^{37} \times T^{-7.40} \times \exp(19\,459.5 / T)$		

These observations have prompted us to examine the unimolecular reactions of the isobutyl radical, which is the basis for branched systems in many detailed kinetic models. In Table 1, we compare rate constants for the unimolecular reactions of isobutyl (R1a, R1b and R1c) from several commonly used and well-vetted kinetics models.[12-15] The branching ratio of $(k_{1b} + k_{1c}) / k_{1a}$ varies between the models by up to a factor of 25 at 1200 K and 101.3 kPa. Some models[6, 13-14] assume isobutene will be produced from C-H β-scission while others[12] assume it's almost entirely from 1,2-H shift isomerization. Westbrook, Mehl, Pitz, and colleagues at the Lawrence Livermore National Laboratory (LLNL) have published multiple models,[13-15] with a range of branching ratios for R1b + R1c, that are typically lower than the other models (C-H scission branching of 10 % or less). Only their toluene and aromatics model[15] includes 1,2-H shift isomerization, but with a rate constant that makes it less important than in AramcoMech 2.0.[12] These variations show that branching ratios of C-H β-scission and 1,2-H shifts should be further clarified to prevent incorrect model predictions of, for example, ignition delay times (which can be sensitive to the branching between C-H and C-C scission[34]) or incorrect analysis of experimental data.

Here, we assess a range of models in the recent literature and carry out experiments with isobutyl to better define its actual behavior. We pyrolyzed dilute mixtures of isopentylbenzene and a radical scavenger in argon to create the isobutyl radical under conditions where it only undergoes unimolecular decomposition, yielding either propene and CH_3 or isobutene and H. The alkene products – quantified post-shock using gas chromatography (GC) with flame ionization (FID) and mass spectrometric (MS) detection – are stable and provided a direct measure of the branching ratio of the competing channels. Uncertainties related to any secondary chemistry were minimized by the dilute conditions and the use of a radical scavenger. Side

chemistry was further probed by varying the mixture composition and employing a kinetics model based on JetSurF 2.0.[6] Experimental results were compared with our adjusted kinetics model and with predictions from the models listed in Table 1.

2. EXPERIMENTAL

2.1 Shock tube with GC/MS detection

All experiments were performed using the National Institute of Standards and Technology (NIST) heated shock tube reactor.[30, 35-37] The reactor and sampling system were maintained at 393 K. Sample gas mixtures containing reactants and radical precursors were prepared in holding tanks and a 150 torr (20 kPa) sample was introduced into the driven section of the shock tube. The driver section was pressurized to (140 to 270) kPa and the shock wave generated by rupture of a cellophane diaphragm separating the driven and driver sections. Shock conditions of (200 to 400) kPa and (950 to 1250) K were created for (500 ± 50) μs prior to re-expansion and cooling.[30, 37] Within a few seconds of the shock, a valve and loop system was used to withdraw a sample of the post-shock gas for quantitative analysis using a Hewlett-Packard 6890N gas chromatograph (GC) equipped with dual flame ionization detectors (FIDs) and an Agilent 5975 mass spectrometer (MS). Neat 1 ml portions at 102.3 kPa pressure were introduced onto two GC columns, a 30 m x 0.53 mm i.d. Restek Rt-Alumina (aluminum oxide porous layer) capillary column for separating species C_5 or less[37] and a 30 m x 0.53 mm i.d. Restek Rtx-1 column for larger molecules. The effluent from the Rtx-1 column was split with an Agilent microfluidic splitter (Dean's Switch) and injected simultaneously into an FID and the MS. The FID detectors were used for product quantification while the MS provided product identification. The GC oven temperature was held at 213 K (-60 °C) for 3 min following injection, then increased by 8 K/min to 383 K (110 °C), then increased by 15 K/min to 473 K (200 °C), and finally held at 473 K for (4 to 14) min.

The sensitivity of the FID to small alkenes was calibrated with a standard alkene mixture (Matheson, 100 μL/L ethene, propene, *n*-butene, *n*-pentene and *n*-hexene in He, concentration accurate to 5 %), as well as hydrocarbon gas mixtures prepared in-house with calibrated manometers. The Matheson standard was measured intermittently during experiments to ensure proper GC/MS function. We estimate that the analytical uncertainty (2 σ) for small hydrocarbons (including propene and isobutene) in our system to be 6 %. This is expected to increase to about 12 % near detection limits, typically about 0.01 μL/L (ppm). We did not have samples for many of the larger aromatic compounds detected in our system, so the analytical uncertainty for these compounds is expected to be higher, approximately 12 %.

Table 2 gives a summary of experimental conditions. We made three different reagent mixtures and performed about 25 individual shocks at different temperatures for each mixture. Each mixture contained isopentylbenzene (Sigma Aldrich, ≥97.0 %) and 1,3,5-trimethylbenzene (Sigma Aldrich, 99 %) diluted with Ar (Matheson, 99.999 % high purity). The 1,3,5-trimethylbenzene was distilled to remove *m*-xylene contaminants, but still contained small amounts of other trimethylbenzene isomers (≤ 0.6% of [1,3,5-trimethylbenzene]) and benzaldehyde (≤ 0.02% of [1,3,5-trimethylbenzene]).

Table 2. Experimental conditions. All concentrations are in μL/L (ppm).

Mixture	Temperature Range (K)	Pressure Range (kPa)	[isopentyl benzene]	[1,3,5-trimethylb enzene]	[chloro cyclo pentane]	[4-vinyl cyclo hexene]	[cyclo hexene]
A	1088 – 1251	243 – 284	385	9085	63	68	-
B	950 – 1125	243 – 375	1705	27470	60	57	-
C	993 – 1226	212 – 405	122	32768	-	54	60

The temperature of the shocked gas was measured with the decomposition of a variety of internal temperature standards (Table 3), including chlorocyclopentane (Sigma Aldrich, 99 %),

4-vinylcyclohexene (Sigma Aldrich, 98 %), and cyclohexene (Sigma Aldrich >99 %). The rate of decomposition of these compounds can be found with first-order kinetics:

$$k_{decomp} = \frac{1}{t}\ln\left(\frac{A_0}{A_t}\right) \quad \text{(E1)}$$

where k_{decomp} is the decomposition rate constant of the standard at the temperature of the shockwave (T_{shock}), t is the time of the shock, (500 ± 50) μs, and A is the integrated peak intensity of the temperature standard before the shock (A_0) or at time, t. The temperature can then be determined using the Arrhenius parameters (E_a and A, where $k_{decomp} = A \times \exp(-E_a/RT_{shock})$ and R is the gas constant) listed in Table 3. Shock pressures were calculated using the ideal shock equation with the temperature of the driver section before the shock, the temperature of the driven section during the shock, and the composition of the mixture.

Table 3. Internal temperature standards

Compound	Decomposition products	Temperature range (K)	$\log_{10}A$ (s^{-1})	E_a/R (K)
isopentylbenzene*	Benzyl + isobutyl	1120 – 1260	16.19	34 215
Cyclohexene	C_2H_4 + 1,3-butadiene	1080 – 1240	15.15[38]	33 514[38]
4-vinylcyclohexene**	2 × 1,3-butandiene	1000 – 1120	14.60[38-39]	29 537[38-39]
Chlorocyclopentane	HCl + cyclopentane	880 – 1020	13.78[39]	24 456[39]

*Value from this work.
** Rate constant for 4-vinylcyclohexene based on the relative rate measurements of Awan *et al*.[39] with the absolute rate derived from cyclohexene decomposition from Tsang (1981).[38] The rate consant for chlorocyclopentane by Awan *et al*.[39] is also relative to the cyclohexene rate constant from Tsang (1981).[38]

2.2 Chemical Modeling

In Section 3 we will show that side chemistry only weakly affects the experimental maximum for the C-H to C-C beta scission ratio, but that it significantly impacts the minimum possible value. To better understand our results, we have created a chemical kinetic model with the Cantera software package.[40] The key chemistry described by our model includes the

unimolecular decomposition of isopentylbenzene, the chemistry of 1,3,5-trimethylbenzene, and the radical-induced decomposition of isopentylbenzene. Most rate constants for small-molecule hydrocarbon reactions were taken from JetSurF 2.0.[6] To these are added additional reactions to describe chemistry of isopentylbenzene and the radical scavenger, 1,3,5-trimethylbenzene; 1,3,5-trimethylbenzene chemistry was previously added to JetSurF by Sheen and coworkers.[29, 41] In Table 4 are shown rate constants for the most important reactions, as defined by a sensitivity analysis (described later in this section) and a reaction path analysis that is in the supplemental information. The reaction path analysis highlights which reactions are important in the production and loss of isobutyl, propene and isobutene. Our full kinetics model is also available in the supporting information.

Some reactions were modeled as reversible, with the reverse rates calculated with the thermochemistry; these reactions have a reversible arrow (↔) in Table 4. Other reactions, mostly those of the larger aromatic compounds, were input as irreversible, because we could not find reliable thermochemistry. For these reactions, we ensured that only the forward reaction is important in our system, usually due to the extremely dilute concentrations of the reactants for the reverse process. To distinguish $C_6H_5C_5H_{10}$ radicals – isopentylbenzene ($C_6H_5C_5H_{11}$) with one H abstracted from reaction with H or CH_3 – we add "*p*-", "*t*-","*s*-", or "*b*-" to denote a the radical center on the primary, tertiary, secondary (not adjacent to aromatic ring) and benzylic carbons, respectively.

Table 4. Key reactions and their rate constants used in the kinetics model. Parameters are for the equation $k = A \times T^n \times \exp(-E_a/RT)$. A is in units of mol, s, cm; E_a/R is in K.

	Reaction		$\log_{10}(A)$	n	E_a/R	Reference
R1a	propene + CH_3 ↔ isobutyl	k_0	28.11	-4.27	1223.4	JetSurF 2.0[6]
		k_∞	13.30	0	5787.0	Curran 2006[1]
R1b + R1c	isobutene + H ↔ isobutyl	k_0	38.80	-6.66	3522.5	JetSurF 2.0[6]
		k_∞	13.24	0	1808.0	Tsang and Walker 1989[42]

R2a	isopentylbenzene → benzyl + isobutyl	k	16.29	0	37 309	This work
R2b	isopentylbenzene → 2-phenyl ethyl + isopropyl	k	16.53	0	49 818	This work
107	2 × CH_3 ↔ C_2H_6[a]	k_∞ k_0	14.38 50.58	-0.34 -10.03	0 1102.6	Blitz *et al*.[43]
1500	*2*-phenylethyl → styrene + H	k	6.579	1.991	16 156	Tokmakov and Lin[44]
1499	*2*-phenylethyl → C_6H_5 + C_2H_4	k	11.235	0.783	19 477	Tokmakov and Lin[44]
R3a	isopentylbenzene + H → *b*-$C_6H_5C_5H_{10}$ + H_2[b]	k	13.92	0	2696.8	Estimate based on JetSurF[6]
	isopentylbenzene + CH_3 → *b*-$C_6H_5C_5H_{10}$· + CH_4[c]	k	11.32	0	3270.9	Estimate based on JetSurF[6]
R3b	isopentylbenzene + H → *s*-$C_6H_5C_5H_{10}$ + H_2[d]	k	6.08	2.4	2249.9	Tsang 1988[45]
	isopentylbenzene + CH_3 → *s*-$C_6H_5C_5H_{10}$· + CH_4[d]	k	-0.29	3.46	2760.2	Tsang 1988[45]
R3c	isopentylbenzene + H → *t*-$C_6H_5C_5H_{10}$ + H_2[e]	k	5.78	2.4	1300.0	Tsang 1990[46]
	isopentylbenzene + CH_3 → *t*-$C_6H_5C_5H_{10}$· + CH_4[e]	k	-0.044	3.46	2314.0	Tsang 1990[46]
R3d	isopentylbenzene + H → *p*-$C_6H_5C_5H_{10}$ + H_2[f]	k	6.08	2.54	3400.0	Tsang 1990[46]
	isopentylbenzene + CH_3 → *p*-$C_6H_5C_5H_{10}$· + CH_4[f]	k	-0.044	3.65	3600.0	Tsang 1990[46]
815	1,3,5-TMB + H ↔ 3,5-dimethylbenzyl + H_2	k	14.07	0	3900	Sheen *et al*. 2013[41]
814	1,3,5-TMB + H ↔ *m*-Xylene + CH_3	k	14.52	0	4300	Sheen *et al*. 2013[41]
1512	1,3,5-TMB + CH_3 → 3,5-dimethylbenzyl + CH_4[g]	k	11.98	0	4780.6	Estimate based on JetSurF[6]
816	1,3,5-TMB ↔ 3,5-dimethylbenzyl + H	k	15.97	0	44 900	Baulch *et al*. 1994[47]
805	benzyl + CH_3 ↔ ethylbenzene	k	13.08	0	111.2	Brand *et al*. 1990[48]
1510	3,5-dimethylbenzyl + CH_3 → EDMB[h]	k	13.08	0	111.2	Brand *et al*. 1990[48]

a. Rate not given in format recognized by Cantera. We fit "fit 5" from the supporting information of Biltz *et al*.[43] to a standard Troe equation (least squares fit) from (800 to 1150) K and (100 to 500) kPa.

b. From reaction 673 of JetSurF, Toluene + H → benzyl + H_2. Scaled to number of labile hydrogens and activation energy decreased by 12.5 kJ/mol because it's a secondary, not primary, carbon.

c. From reaction 676 of JetSurF, Toluene + CH_3 → benzyl + CH_4. Scaled to number of labile hydrogens and activation energy decreased by 12.5 kJ/mol because it's a secondary not primary, carbon.

d. D Rate constant originally for H abstraction from the secondary carbon of *n*-butane.

e. B Rate constant originally for H abstraction from the tertiary carbon of isobutene.

f. C Rate constant originally for H abstraction from the primary carbon of isobutene.

g. G From reaction 676 of JetSurF, Toluene + CH_3 → benzyl + CH_4. Scaled to number of labile hydrogens.

h. H Same rate constant as benzyl + CH_3.

Our simulation accounts for chemistry during and after the shock. First, the simulation temperature was held at the temperature of the shock, T_{shock}, for 500 μs. The post-shock temperature decay was then modeled with 4 isothermal time steps that approximate the temperature decrease of the experimental shock: 250 μs at 0.875 T_{shock}, 250 μs at 0.75 T_{shock}, 500 μs at 0.5 T_{shock}, and 1 s at 393 K (the wall temperature of the shock tube). The simulation held the number density of the gas constant, so pressure decreased with temperature. As later discussed (section 4.2), the concentrations of most species of interest, including isobutene and propene, were unaffected by post-shock chemistry. The simulation assumed that the beginning of the shock produced (independent of temperature) 1 μL/L of H atoms, to approximately match *m*-xylene concentrations (as described in section 3.1, *m*-xylene is a tracer for H atoms) at low temperatures. This accounts for a small number of radicals produced from unknown sources.

We identified key model reactions, listed in Table 4, with a sensitivity analysis using the MUM-PCE 0.1 software package published by Sheen.[49-52] Sensitivities are defined by equation (E2), wherein $S_{m,i}$ is the sensitivity of η_m – the model prediction of a species concentration or ratio of species in the shock tube – to the *i*th rate constant, θ_i :

$$S_{m,i} = \frac{d\eta_m}{d\theta_i}\frac{\theta_i}{\eta_m} \qquad \text{(E2)}$$

The derivative in the above equation is computed by calculating η_m using the kinetics model and with the *i*th rate constant increased by 1 %. While the kinetics model includes 1523 different rate constants, most reactions are unimportant to the output of the model, η_m, either because they are too fast to be a rate limiting reaction, are too slow to be competitive with product-forming steps, or don't involve key species in the shock tube. We tested the sensitivity of the model to eleven experimentally observed species: methane, ethane, ethylene, ethylbenzene, 1-ethyl-3,5-

dimethylbenzene (EDMB), propene, isobutene, benzene, toluene, *m*-xylene and styrene. With a sensitivity cutoff of 5 % of the maximum sensitivity for any reaction, we found 28 reactions to affect modeling of at least one of the eleven target species. This decreased to only 14 reactions when just considering the ratio of propene to isobutene; all 14 of these reactions are included in Table 4.

The rate constants for these key reactions were optimized manually to match the experimental results, with choices derived from a critical analysis of information from the literature and present experiments. Our rate constant choices and adjustments will be described in the modeling results section (section 4.1).

We also compared our data to commonly used kinetics models: JetSurF 2.0 (unmodified)[6], AramcoMech 2.0[12] and LLNL.[13-15] For these models, we did not modify any parameters or rate constants for isobutyl, but added any necessary isopentylbenzene and 1,3,5-trimethylbenzene chemistry, with associated rates taken from our modified JetSurF 2.0 model unless otherwise indicated. LLNL provides many different models, but all our LLNL mechanisms were based on their "toluene, ethyl-, propyl, & -butyl benzene" model[15] because it contained much of the necessary aromatic chemistry. We will call this model "LLNL aromatics." In this model, 1,3,5-trimethylbenzene chemistry was assumed to have the same rate constants as toluene in the LLNL model, but scaled appropriately to the number of labile -CH_3 or -H groups. There are two other rate constants for the decomposition of isobutyl (R1) among the LLNL mechanisms (Table 1). We substituted these rate constants into the LLNL aromatics model to make the "LLNL isooctane" model (with rate constants for R1 typically used in the LLNL alkane mechanisms) and "LLNL biodiesel" (with rate constants for R1 typically used in mechanisms published in 2010 or earlier).

3. EXPERIMENTAL RESULTS

3.1 Product Distributions

Scheme 2. *The decomposition of isopentylbenzene.*

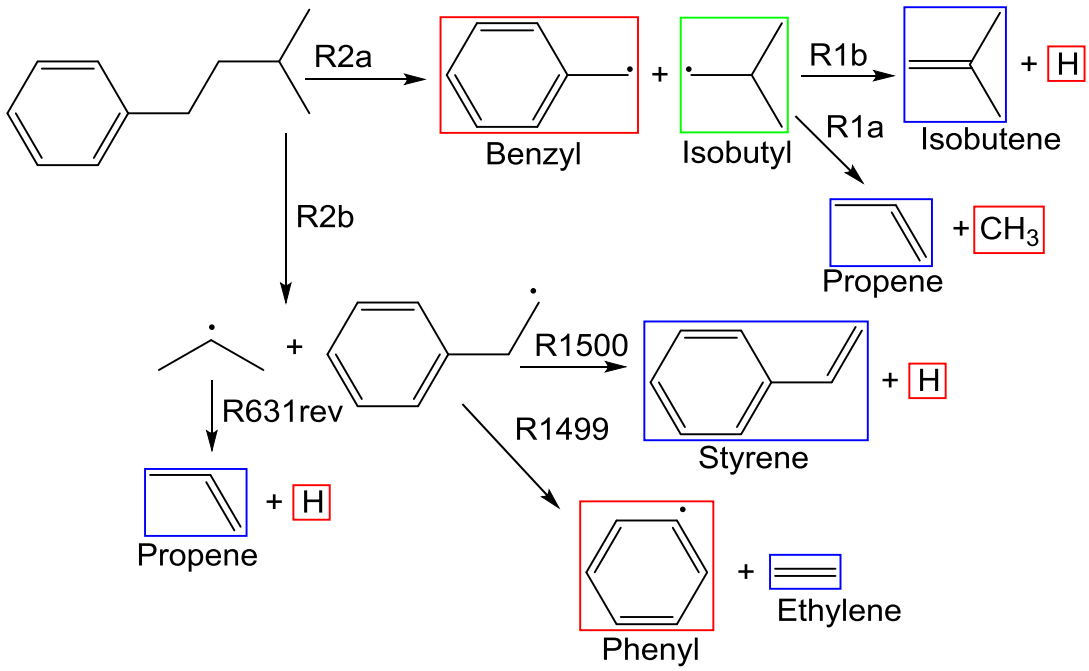

The goal of our experiment was to create the isobutyl radical – from the pyrolysis of isopentylbenzene, R2a in

Scheme ***2*** – under dilute conditions where it undergoes only unimolecular decomposition (since the lifetime of isobutyl is expected to be less than 1 μs under our conditions,[6, 12, 15] we predict that less than 0.1 % of isobutyl undergoes bimolecular reaction with the inhibitor or other species) and then to observe the stable alkene products to deduce the cracking pattern. To test for systematic experimental errors, we varied the concentration of isopentylbenzene by a factor of 14, the concentration of radical scavenger by a factor of 3.5, and the ratio of scavenger to isopentylbenzene from 16 to 270. Product tables for all mixtures are in the supporting information. The products of five selected shocks from mixture C are given in Table 5, which lists all compounds detected at concentrations about 1 % or greater of propene (excluding

products from the temperature standards). Concentrations of the 10 most abundant products (methane < propene < toluene < 1-ethyl-3,5-dimethylbenzene (EDMB) < ethylbenzene < styrene < *m*-xylene < ethane < isobutene < benzene) for mixture B are shown as a function of temperature in Figure 1.

Table 5. Products with the 10 highest concentrations for 5 select shocks from mixture C. All concentrations in μL/L.

T (K)	p (kPa)	C_3H_6	CH_4	Toluene	EDMB	*m*-xylene
1045	272	0.400	0.771	0.105	0.00819	0.124
1097	303	2.03	2.76	0.632	0.123	0.652
1121	329	4.02	5.23	1.41	0.346	1.17
1155	357	16.7	18.1	7.02	2.42	3.72
1194	383	37.2	37.6	17.2	7.35	8.24

T (K)	p (kPa)	Styrene	Ethyl-benzene	Benzene	$isoC_4H_8$	Ethane
1045	272	0.0911	0.000	0.0119	0.0109	0.000
1097	303	0.388	0.132	0.109	0.0502	0.0469
1121	329	0.509	0.303	0.245	0.0959	0.0818
1155	357	2.24	1.12	1.28	0.331	0.312
1194	383	4.41	2.48	2.40	0.749	0.691

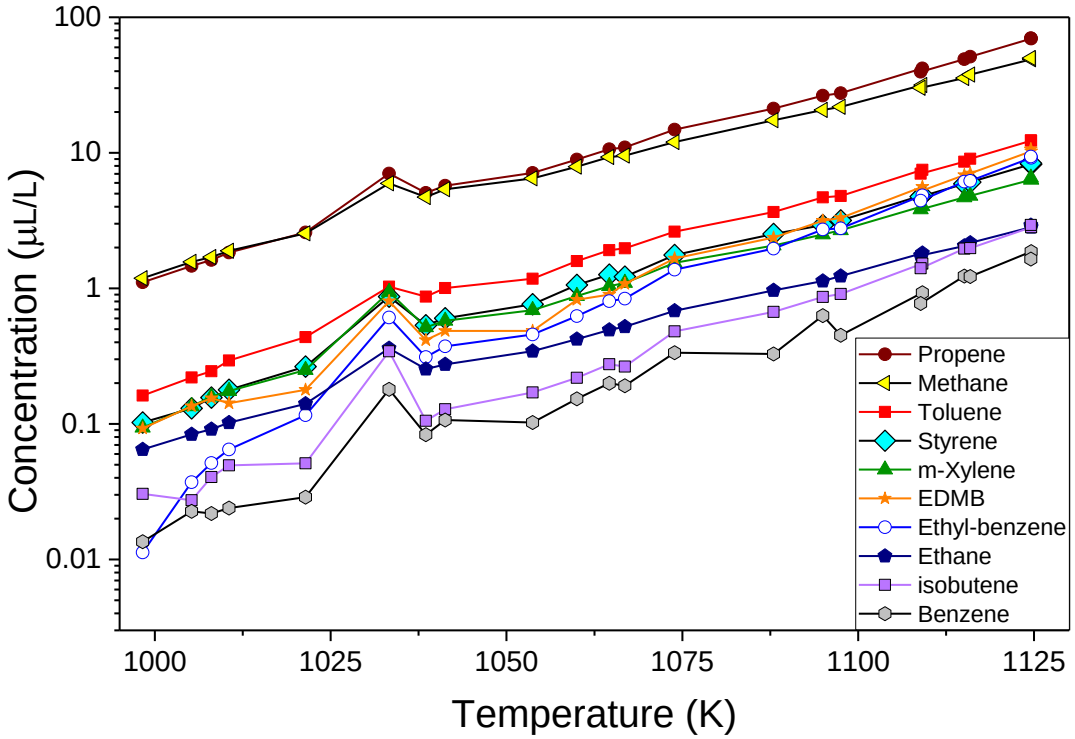

Figure 1. Products of mixture B as a function of temperature.

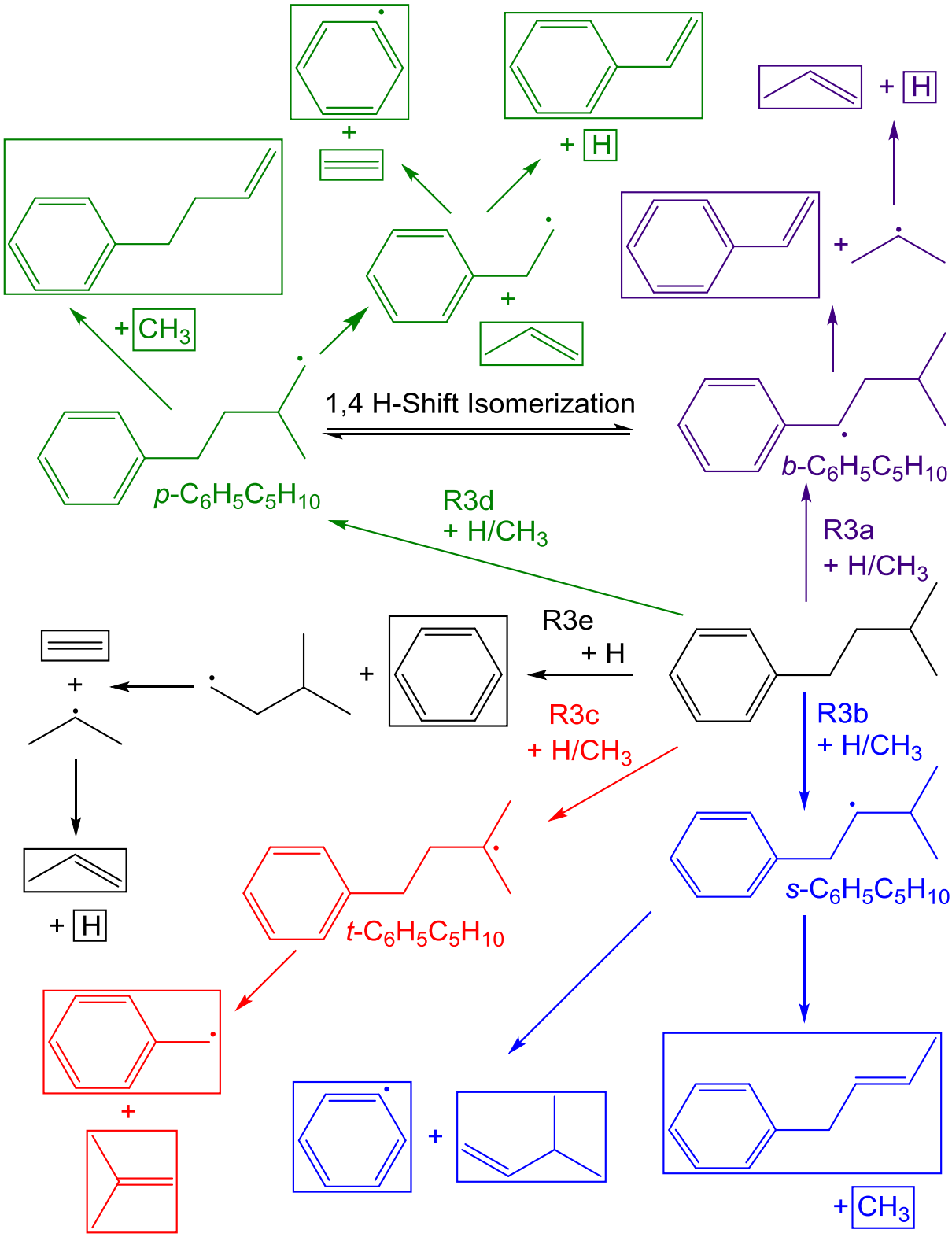

Scheme 3. Possible radical attack on isopentylbenzene by H and CH_3. For $C_6H_5C_5H_{10}$ – isopentylbenzene with one H abstracted – the prefixes "*p*-", "*t*-", "*s*-" and "*b*-" denote a radical center on the primary, tertiary, secondary and benzyl carbons, respectively.

The two most abundant products are propene and methane. Propene is primarily formed from the C-C β-scission of isobutyl radicals (R1a in Scheme 1), and methane is the main product of the CH_3 formed stoichiometrically in the same reaction. Methyl radicals can also be produced by a variety of side reactions (Scheme 2 and Scheme 3), resulting in methane concentrations that are slightly higher than those of propene. We also observed small amounts of ethane, produced primarily from the self-recombination of methyl radicals.

$$CH_3 + CH_3\ (+M) \leftrightarrow C_2H_6\ (+M) \qquad \text{(R107)}$$

Little isobutene is observed – one to two orders of magnitude less than propene – indicating that few isobutyl radicals decompose via C-H scission (R1b) or 1,2 H-shift isomerization (R1c). Both R1b and R1c lead to the same product, isobutene, so our experiment measures the combined branching ratio of these two channels, $(k_{1b} + k_{1c})/k_{1a}$. We will often refer to the two channels that make isobutene together as R1b + R1c.

The next most abundant products observed are toluene, ethyldimethylbenzene (EDMB) and ethylbenzene, all likely from the chemistry of benzylic radicals (i.e. benzyl and substituted benzyl species). Benzylic radicals are produced in large quantities from the decomposition of isopentylbenzene (R2a in Scheme 2, yielding benzyl) or from the reaction of H and CH_3 with 1,3,5-trimethylbenzene:

$$\text{1,3,5-trimethylbenzene} + H \rightarrow \text{3,5-dimethylbenzyl} + H_2 \qquad \text{(R815)}$$

$$\text{1,3,5-trimethylbenzene} + CH_3 \rightarrow \text{3,5-dimethylbenzyl} + CH_4 \qquad \text{(R1512)}$$

Due to resonance stabilization, the benzylic radicals produced from R2a, R815 and R1512 are stable at our temperatures and do not readily abstract H from closed shell species; they primarily recombine with other radicals. Recombination of benzyl radicals with CH_3 accounts for the observed ethylbenzene and EDMB:

$$\text{benzyl} + CH_3 \rightarrow \text{ethylbenzene} \quad \text{(R805)}$$

$$\text{3,5-dimethylbenzyl} + CH_3 \rightarrow \text{EDMB} \quad \text{(R1510)}$$

Benzyl radicals from R2a can also react with 1,3,5-trimethylbenzene to produce the observed toluene (Figure 1 and Table 5):

$$\text{benzyl} + \text{1,3,5-trimethylbenzene} \rightarrow \text{3,5-dimethylbenzyl} + \text{toluene} \quad \text{(R1511)}$$

The reaction of 1,3,5-trimethylbenzene with H can produce *m*-xylene via R814. *m*-Xylene was always observed, but in smaller concentrations than most of the other aromatic products, like toluene and ethylbenzene.

$$\text{1,3,5-trimethylbenzene} + H \rightarrow m\text{-xylene} + CH_3 \quad \text{(R814)}$$

Since most H radicals react with 1,3,5-trimethylbenzene (because of its large excess) and the rate constant for R814 is known,[41, 53] *m*-xylene is a tracer for H chemistry. The observed *m*-xylene concentration was typically (5 to 15) times lower than the sum of all products of methyl chemistry ($CH_4 + 2\times C_2H_6$ + EDMB + ethylbenzene). This indicates a low flux of H and, since H is typically more reactive than CH_3, a low concentration of H in the shock tube. This is consistent with the expectation that R1b + R1c, which make H, is unfavorable compared to R1a. The kinetics model supports this conclusion, predicting H concentrations (100 to 4000) times lower than CH_3 concentrations.

We detected styrene and benzene, typically at concentrations 10 % and 3 % of the propene concentration, respectively. A minor decomposition pathway of isopentylbenzene (R2b, Scheme 2) will produce 2-phenylethyl, which can then decompose to make either styrene or benzene (R1500 and R1499, Scheme 2). Styrene and benzene can also be formed from H and CH_3 attack on isopentylbenzene (R3a, R3b, R3d and R3e, Scheme 3). Except for R3b, all of these side reactions produce propene as a coproduct of styrene or benzene, so subtracting styrene

and benzene from the propene concentration accounts for most known propene-producing side chemistry. This is typically a (10 to 15) % correction to the total propene concentration and – except for experiments with very low isopentylbenzene decomposition, < 3 ppm – never more than a 20 % correction. There is no similar way correct for secondary sources of isobutene, like R3c. Potential secondary isobutene will be shown (Section 4.2) to be the major cause of uncertainty in the minimum possible value of the C-H to C-C beta scission ratio.

We detected small amounts of isopropyl-benzene; isopropyl-methylbenzene; phenylbutene; 1-butene; 2-butene; dimethylstyrene; C_5 compounds, which are likely isomers of pentene and pentane; acetylene; and allene. Typically, these species were less than 1 % of the abundance of propene. At lower temperatures (<1050 K) where secondary chemistry is most important, these species each comprise a maximum of 5 % of the propene concentration. Phenylbutene is a marker compound for H and CH_3 attack on isopentylbenzene (Scheme 3), and allows estimation of the extent of these reactions (R3). We typically detected phenylbutene at concentrations 0.5 % or less of the propene concentration (the only exception is very low temperature experiments for mixture B). Mixture C – the mixture with the highest concentration of scavenger – had phenylbutene concentrations of 0.1 % or less of propene concentration. This indicates that radical attack on isopentylbenzene is minimal in our system. While bibenzyl (from R820) was detected in small amounts, we did not see any other bibenzylic species (from R1522 and 1523), probably because these compounds are too large to elute from our columns.

$$\text{benzyl} + \text{benzyl} \rightarrow C_6H_5CH_2\text{-}CH_2C_6H_5 \qquad \text{(R820)}$$

$$\text{3,5-dimethylbenzyl} + \text{3,5-dimethylbenzyl} \rightarrow C_{18}H_{22} \qquad \text{(R1522)}$$

$$\text{3,5-dimethylbenzyl} + \text{benzyl} \rightarrow C_{16}H_{18} \qquad \text{(R1523)}$$

The bibenzyl detected, consequently, gives qualitative but not quantitative evidence of formation of other bibenzylic products.

Traces of a pentane and a pentene were identified by MS analysis and are probably isopentane and isopentene, which are likely from either the R3b or from the recombination of isobutyl with CH_3:

$$iC_4H_9 + CH_3 \rightarrow iC_5H_{12} \qquad \text{(R1517)}$$

The abundance of these compounds was 1 % or less than that of propene. This indicates that the decomposition lifetime of isobutyl is small enough to preclude much recombination (R1517). A reaction path analysis is available in the supporting information for the kinetics model, which includes various isobutyl recombination reaction, none of which compete with R2a. The low pentene and pentane concentrations also provide more evidence that secondary radical attack on isopentylbenzene is minimal.

We also detected the decomposition products of our temperature standards: cyclopentene and small amounts of cyclopentadiene from chlorocyclopentane decomposition; 1,3-butadiene from 4-vinylcyclohexene decomposition; and 1,3-butadiene and ethene from cyclohexene decomposition.

3.2 Kinetics of Isopentylbenzene Decomposition

Figure 2 shows an Arrhenius plot for the unimolecular decomposition of isopentylbenzene. The rate of total isopentylbenzene decomposition, $k_{2,total}$, is calculated from the total loss of isopentylbenzene (E3), whereas k_{R2a} (the rate of only R2a) is calculated from the production of propene and isobutene (E4):

$$k_{2,total} = \frac{1}{t} \times \ln\left(\frac{[\text{isopentylbenzene}]_0}{[\text{isopentylbenzene}]_t}\right) \qquad \text{(E3)}$$

$$k_{2a} = \frac{1}{t} \times \ln\left(\frac{[\text{isopentylbenzene}]_0}{[\text{isopentylbenzene}]_0 - [\text{propene}]_{t,R2a} - [\text{isobutene}]_t}\right) \quad \text{(E4)}$$

$$[\text{propene}]_{t,R2a} = [\text{propene}]_t - [\text{styrene}]_t - [\text{benzene}]_t$$

where t is the shock time (500 μs). The subscript "0" indicates initial concentration (before the shock), and the subscript "t" indicates concentration at time, t. The subscript "R2a" was added to [propene], because measured styrene and benzene concentrations were subtracted from the propene concentration to correct for side chemistry, especially reaction R2b. Tables of individual rate constants for all experiments are given in the supporting information. An Arrhenius fit to the propene formation data calculated with equation E4 (Figure 2) gives the rate constant for reaction R2a (all uncertainties given in this section are 2 σ):

$$k_{2a} = 10^{16.29 \pm 0.37} \times \exp(-(37\,300 \pm 900)\ \text{K} / \text{T})\ \text{s}^{-1}$$

$$950\ \text{K to } 1225\ \text{K}$$

This rate constant is very close to the decomposition rate constant of *n*-pentylbenzene found by Walker and Tsang[54] of $1 \times 10^{16} \exp(-36\,500\ \text{K} / \text{T})\ \text{s}^{-1}$, which is also plotted in Figure 2. Both reactions involve breaking a C-C bond to make benzyl radical and a primary radical, so their rate constants should be similar. The agreement in these rate constants is strong confirmation of the mechanism and suggests that we have accounted for all significant sources of propene.

The total rate constant, $k_{2,total}$ is found by fitting experimental data for total isopentylbenzene loss ($k_{2,total}$, equation E3) to the Arrhenius equation:

$$k_{2,total} = 10^{16.42 \pm 0.80} \times \exp(-(37\,400 \pm 2200)\ \text{K} / \text{T})\ \text{s}^{-1}$$

$$1050\ \text{K to } 1225\ \text{K}$$

In Figure 2 we only include points for $k_{2,total}$ with ≥10 % isopentylbenzene loss; at lower conversions (temperatures) these data are noisy and unreliable because the change in the *n*-pentylbenzene concentration becomes comparable to our analytical precision. The determined

rate parameters for $k_{2,total}$ has a high uncertainty because only seven shocks had isopentylbenzene decomposition above 10 % and the temperature range is narrow. The rates of R2a (equation E4) are slightly lower than the total rate (E3). The difference between the two rates is about 15 % between (1150 and 1225) K, indicating that about 15 % of the isopentylbenzene is lost to reaction R2b or radical reactions. Assuming low amounts of radical attack on isopentylbenzene, we can find k_{2b} by subtracting k_{2a} from $k_{2,total}$, and this data is plotted on the bottom panel of Figure 2 (black squares). Fitting this data gives:

$$k_{2b} = 10^{(17.0 \pm 5.6)} \times \exp(-(41\,000 \pm 15\,000)\ \mathrm{K} / \mathrm{T})\ \mathrm{s}^{-1}$$

$$1050\ \mathrm{K}\ \text{to}\ 1225\ \mathrm{K}$$

k_{2b}, can also be calculated from the sum of styrene and benzene concentrations at high temperatures, >1080 K. This method (E5) also assumes under these conditions that the only source of styrene and benzene is reaction R2b (no reaction R3).

$$k_{2b} = \frac{1}{t} \times \ln\left(\frac{[\text{isopentylbenzene}]_0}{[\text{isopentylbenzene}]_t - [\text{styrene}]_t - [\text{benzene}]_t}\right) \qquad \text{(E5)}$$

This data is plotted in the bottom panel of Figure 2 (red circles), and an Arrhenius fit to this data results in the following rate expression for R2b:

$$k_{2b} = 10^{(15.9 \pm 1.6)} \times \exp(-(38\,000 \pm 4000)\ \mathrm{K} / \mathrm{T})\ \mathrm{s}^{-1}$$

$$1080\ \mathrm{K}\ \text{to}\ 1225\ \mathrm{K}$$

This value for k_{2b} agrees within uncertainty with the value found by subtracting k_{2a} from k_{total}. If there were secondary production of styrene or benzene (for example reaction R3a), we would expect non-linear behavior for the Arrhenius plot; however, the Arrhenius plot is linear. To additionally ensure low interference from side chemistry, the above value for k_{2b} was fitted only to data from mixture C with temperatures above 1080 K, because, based on our model, this data

is expected to have little side chemistry (R3). The kinetics model predicts that over 92 % of styrene and over 98 % of benzene are from R2b under these conditions.

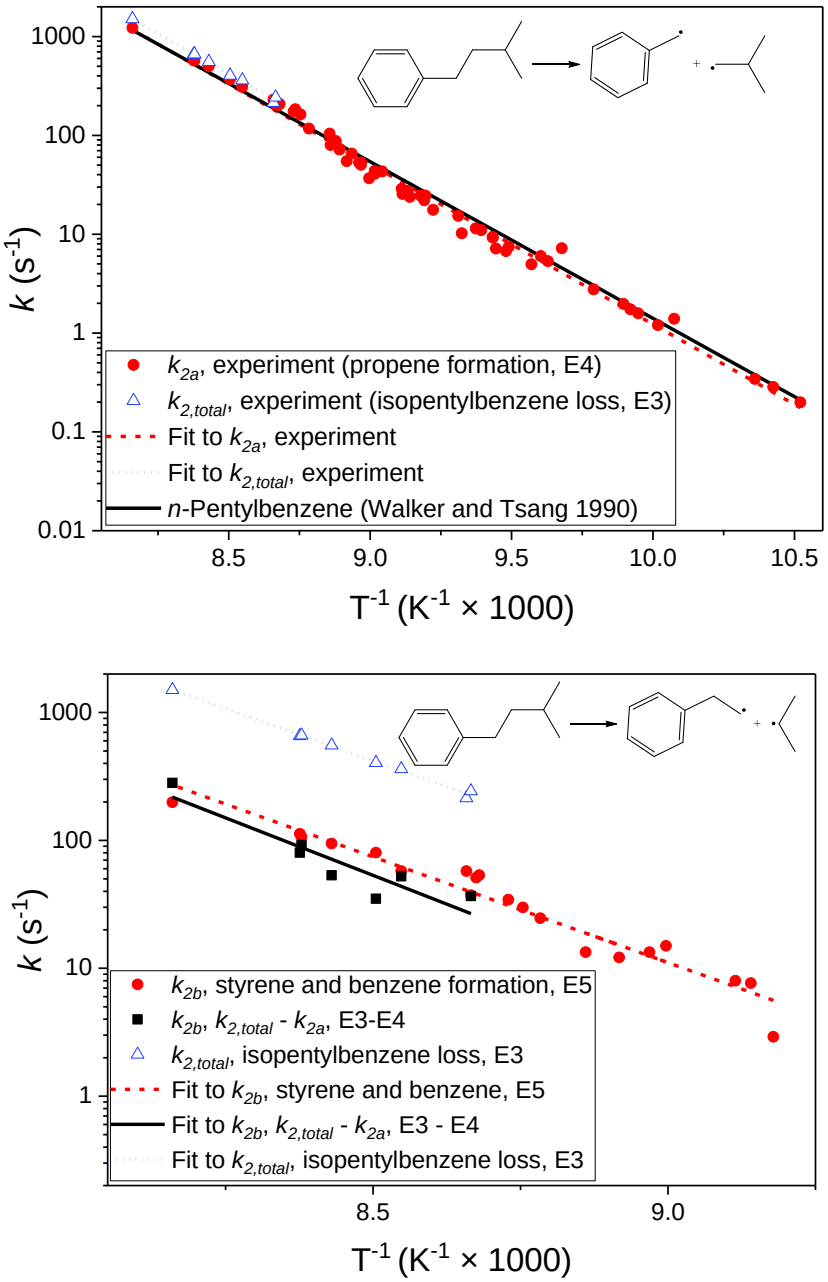

Figure 2. Rate constants for decomposition of isopentylbenzene compared to literature values for *n*-pentylbenzene.[54] The top panel features the rate constants for R2a (red circles), calculated from the formation of propene and isobutene (equation E3) and their Arrhenius fit (dashed red line). The bottom panel features the rate constants for R2b (red circles from equation E5, black squares from the difference between equations E3 and E4) and their Arrhenius fits (dashed red line and solid black line). The total rate constant (blue triangles from equation E3) is shown in both panels with its Arrhenius fit (blue dotted line).

3.3 Isobutene/Propene Ratios

Experiments with all mixtures show propene to be formed in much larger (15 × to 50 ×) concentrations than isobutene, indicating that β-scission of the C-C bond is much faster than ejection of H. The combined branching ratio of R1b + R1c is given by:

$$\frac{k_{1b}+k_{1c}}{k_{1a}} \leq \frac{[\text{isobutene}]}{[\text{propene}]-[\text{styrene}]-[\text{benzene}]} \qquad \text{(E6)}$$

Per previous discussion, subtracting out styrene and benzene from the propene concentration is a small correction to account for side chemistry from R2b, R3a, R3d and R3e.

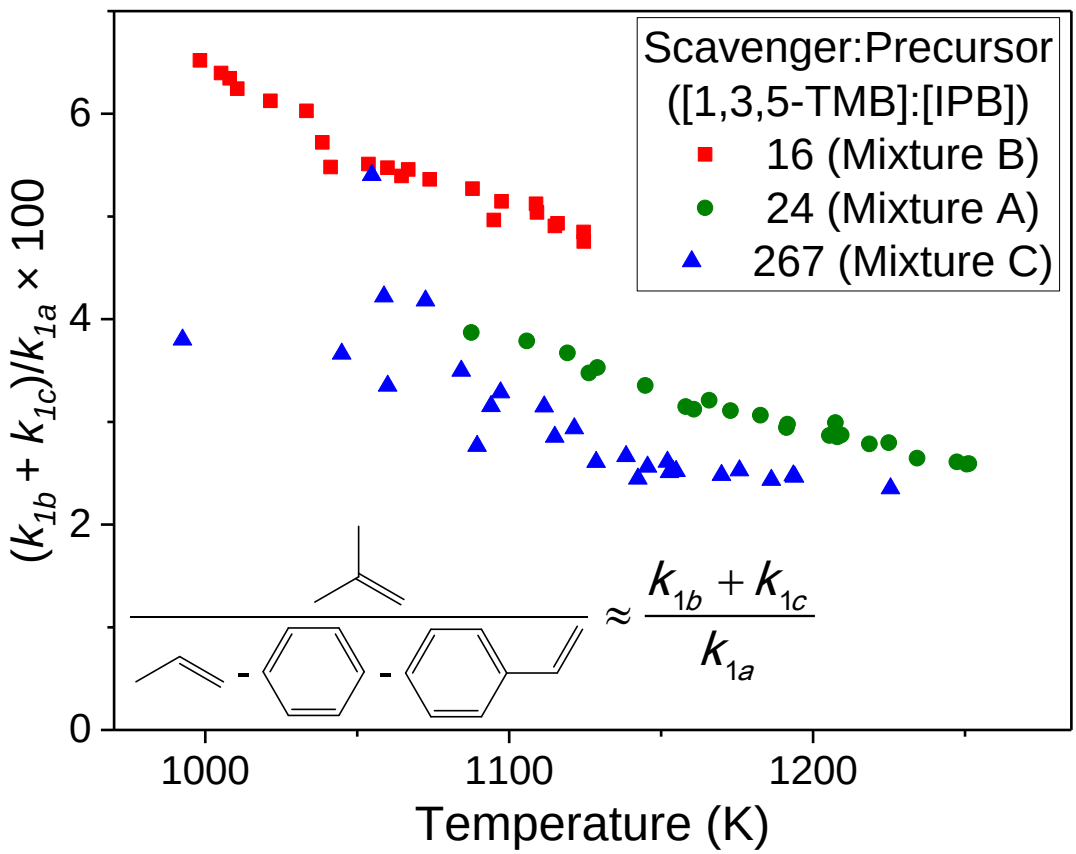

Figure 3. Experimental values of $(k_{1b} + k_{1c})/k_{1a}$ calculated with equation E6 as a function of temperature for all mixtures. Experimental values are expected to have contributions from unaccounted-for side chemistry. 1,3,5-TMB = 1,3,5-trimethylbenzene. IPB = isopentylbenzene.

Experimental values of $(k_{1b} + k_{1c})/k_{1a}$, from equation E6 are plotted in Figure 3. The ratio decreases slightly with temperature and shows up to a factor of 1.7 systematic variation with the

mixture, a result we believe is caused by secondary isobutene sources, e.g. from radical-induced decomposition of isopentylbenzene (Scheme 3). As shown in Figure 3, we measured a ratio of about 5 % at 1100 K when there was 16 times as much radical scavenger as isopentylbenzene. This decreased to about 4 % when there was 24 times as much radical scavenger, and further decreased to about 2.5 % when there was 267 times as much radical scavenger. The branching fraction of R1b + R1c should increase with temperature because of its higher activation energy compared to R1a. The data in Figure 3 show the opposite trend, likely because side chemistry – for example the H abstraction reactions in Scheme 3 – will be proportionally more important at the lower temperatures in which very little isopentylbenzene decomposes.

As shown in Figure 3, the ratio for mixture C is nearly temperature independent above 1150 K with a value of (2.5 ± 0.1) % (2 σ standard deviations, from experimental scatter). This is our best experimental estimate for $(k_{1b} + k_{1c})/k_{1a}$, because we expect the least side chemistry under these conditions: high temperatures and high radical scavenger concentrations. Since it is unclear how much isobutene is directly from isobutyl decomposition even in mixture C, this value is best interpreted as an upper limit for the branching ratio of R1b + R1c.

4. CHEMICAL MODELLING RESULTS

4.1 Choice of Rate Constants

The model includes our best estimates of rate constants based on literature values and sometimes (the decomposition of isopentylbenzene, for example) our experimental data. Table 4 summarizes the rate constants of the main reactions.

JetSurF 2.0[6] gives both R1a and R1b in terms of the reverse reaction and calculates the β-scission reactions by using detailed balance and thermodynamics ($K_{eq} = k_{forward}/k_{reverse}$). The only experimental value of the reverse of R1a (i.e. k_{-R1a}, CH_3 addition to the central carbon of

propene) appears to be the 1987 measurement of Baldwin *et al.*,[55] which was taken at 753 K, temperatures much lower than those of our experiments. There appears to be only a single experimental study of the R1a forward reaction,[56] and it is early work at much lower temperatures. At 1100 K, literature rate constants for R1a vary by about a factor of four: high-pressure rates constants calculated from thermodynamics by Curran[1] are 20 % faster than *ab initio* and RRKM calculations from Knyazev and Slagle,[7] a factor of two faster than rates from *ab initio* and transition state theory calculated rates by Ratkiewicz[57] and a factor of four faster than early experiments by Metcalfe and Trotman-Dickenson.[56] We adjusted the high pressure limit until the rate constants of R1a matched theoretical values of Curran.[1] As the fastest value, the Curran rate constant better matched the experimental data for $(k_{1b} + k_{1c})/k_{1a}$.

For R1b, JetSurF assumed that rate of the reverse reaction (H + isobutene → isobutyl) has the same rate constant as the reaction of H with propene to make *n*-propyl. JetSurF 2.0 does not include the 1,2-H shift isomerization, R1c, so the rate for R1b in the model was assumed to include both mechanisms, R1b and R1c. There is only one experimental measurement for the reaction of H + isobutene to make isobutyl (R1b reverse), the 1989 work of Tsang and Walker,[42] who – also using the NIST shock tube – measured the displacement rate constant (H + isobutene → isobutyl → propene + CH_3) relative to a reference reaction and argued that the displacement and addition rates are nearly identical. Since their high-pressure rate constant is within 15 % of JetSurF 2.0, we chose to use their value for k_∞ with k_0 and Troe parameters from JetSurF.

Rate constants for the unimolecular decomposition of isopentylbenzene, R2a and R2b, are the experimental values from this work (discussed in section 3.2), with k_{2a} calculated from the formation of propene and isobutene (E3) and k_{2b} from the formation of styrene and benzene (E5). To check our experimental value for the rate constant of R2b, we additionally estimated

this rate constant using thermodynamically-based estimates of the bond energy[58] and concluded that the experimental value is physically reasonable. The kinetics model also includes thermodynamically-based estimates of bond-fissions involving the stronger bonds in isopentylbenzene. The results indicate that such decompositions are not significant at the temperatures of this study. The kinetics model suggests the majority of isopentylbenzene decomposition (~85 % at 1100 K and ~80 % at 1200 K) will be via fission of the benzylic C-C bond, R2a, with 15 % to 20 % decomposition from R2b (See reaction path analysis in supporting information).

There is no experimental data for the decomposition of the 2-phenylethyl (R1499 and R1500) produced from R2b, so we adopt the high level quantum and RRKM theory calculations performed by Tokmakov and Lin.[44] They predict approximately 70 % of 2-phenylethyl will decompose to styrene and H atoms and 30 % will decompose to phenyl (C_6H_5) and ethene. This theoretical branching ratio agrees with the experimental data, since we always measured at least double the amount of styrene compared to benzene. For mixture C, the kinetics model with rate constants from Tokmakov and Lin, predicts both the sum of styrene and benzene and the ratio of styrene to benzene to better than 50 %, with a typically difference between the experiment and the model under 20 %

None of the rates of H or CH_3 hydrogen abstraction (Scheme 3) from isopentylbenzene have been studied, but accurate estimations are possible with analogies to similar compounds. For H and CH_3 attack on the primary, secondary and tertiary carbons of isopentylbenzene we adopt rate constants from review articles by Wing Tsang.[45-46] We assume that the tertiary and primary H's of isopentylbenzene are abstracted with rates identical to analogous attack on isobutane.[46] The rate of H abstraction of the secondary carbon by H and CH_3 was assumed to be

identical to abstraction reactions from the secondary carbon of propane. The rate constants were scaled to the number of labile H's. We assume H substitution with isopentylbenzene (R3e) occurs with the same rate constant as H substitution with toluene, and use the rate constant from the updated analysis from Sheen *et al*.[41] for the data from Robaugh and Tsang.[53] Since there were no rate constants for reactions analogous to R3a, we modified the JetSurF 2.0[6] rate constants for H and CH_3 + toluene to make benzyl radical, scaling for the number of labile hydrogens and decreasing the activation energy by 12.5 kJ/mol to account for the reduced bond strength of the secondary benzylic hydrogens compared to primary.

The rate constants for H + 1,3,5-trimethylbenzene are from Sheen *et al*.[41] Abstraction (R815) is more favorable than substitution (R814) by a ratio of about 2:1.[53, 59] Uncertainties in the absolute rate constants are expected to be about a factor of 1.5. The absolute rate constants agree with literature values for toluene + H (multiplied by 3 to account for the number of methyl groups on the aromatic ring) to within a factor of 2 for the temperature range of this study.[47, 60-62] They are also within 30 % of the values in JetSurF 2.0 for the reaction of toluene with H and within 30 % of previous work by Robaugh and Tsang.[6, 53] The rate of 1,3,5-trimethylbenzene reaction with CH_3 was found by scaling the JetSurF rate constant for CH_3 + Toluene[6] to the number of labile H's. Rate constants for 1,3,5-trimethylbenzene decomposition were similarly derived from the JetSurF 2.0 toluene rate constants,[6] based on the work of Baulch *et al*.[47]

$$\text{1,3,5-trimethylbenzene} \rightarrow \text{3,5-dimethylbenzyl} + \text{H} \qquad \text{(R816)}$$

This rate constant is within a factor of two of most other literature values.[48, 63-65]

While the specific recombination reactions of interest, like R805 and R1510, have not been extensively studied, recombination rates are generally well known and show only modest variation.[47] For R805 we use the value of Brand *et al*.,[48] which is the only measurement

available, and adopt an identical value for 3,5-dimethylbenzyl + CH_3. Rates for recombination with H are derived from the thermochemistry and the reverse bond fissions. We include several other reactions of benzylic radicals in our model, including self-reactions to make bi-benzylic species, benzylic H exchange, and recombination with isobutyl. We use methyl recombination rate constants from the 2015 review of Blitz *et al*. [43] They gave full temperature and pressure dependent rate constants, but not in a form compatible with Cantera. We plotted their predicted values from (1 to 5) bar and (800 to 800 to 1150) K and fitted to the Troe equation[66] to get the parameters used in the kinetics model.

Table 6. Reactions updated to match experimental data and their rate constants

Can#	Reaction		$\log_{10}(A)$	n	E_a/R
572	isobutene + H ↔ isobutyl[a]	k_0	38.20	-6.66	3522.5
		k_∞	13.30	0	1808.0
1494	isopentylbenzene + CH_3 → *t*-$C_6H_5C_5H_{10}$· + CH_4[b]	k	0.26	3.46	2314.0

Some modifications were made to the initial model to improve the fit to experiment. While limited knowledge about many rates would allow extensive changes, we elected to alter as few rate constants as possible (Table 6) in order to avoid models that matched the data, but did not make physical sense. Adjustments were made manually, mainly based on the data for mixture C (Figure 3), which should have the least side chemistry due to its high concentration of radical scavenger. We decreased the rate constant for R1b – whose high pressure limit is not from JetSurF, but from Tsang and Walker[42] as shown on Table 4 – to match the measured concentration of isobutene at high temperatures (where there is less side chemistry), lowering the A-factor for k_0 from 6.26×10^{38} cm^6 mol^{-2} s^{-1} to 1.6×10^{37} cm^6 mol^{-2} s^{-1}. This translates to a factor of four decrease in the rate constant under typical conditions of our experiment: 1100 K and 200 kPa. Rather than increasing R1a (high-pressure limit from Curran, Table 4), we decreased the rate of R1b + R1c, because lowering the latter better matched the data. This choice

is also based on theoretical work[67] that predicts that a unimolecular reaction will have much steeper fall-off behavior when it competes with a more favorable (lower activation energy) unimolecular reaction (in this case R1a). We chose to keep the high pressure limit unchanged because there are better literature estimates and experimental data available for k_∞[46] than for k_0. Finally, we increased by a factor of two the A factor of R1494 (CH_3 abstraction from the tertiary site of isopentylbenzene) to better match preliminary data from our group on the reaction of isobutane with H.[68]

4.2 Simulation and Comparison with the Experimental Results

The kinetics model (Table 4) was used to (1) check assumptions we made about our chemistry, (2) find which rate constants and reactions were the most important to our system and (3) compare with experimental data.

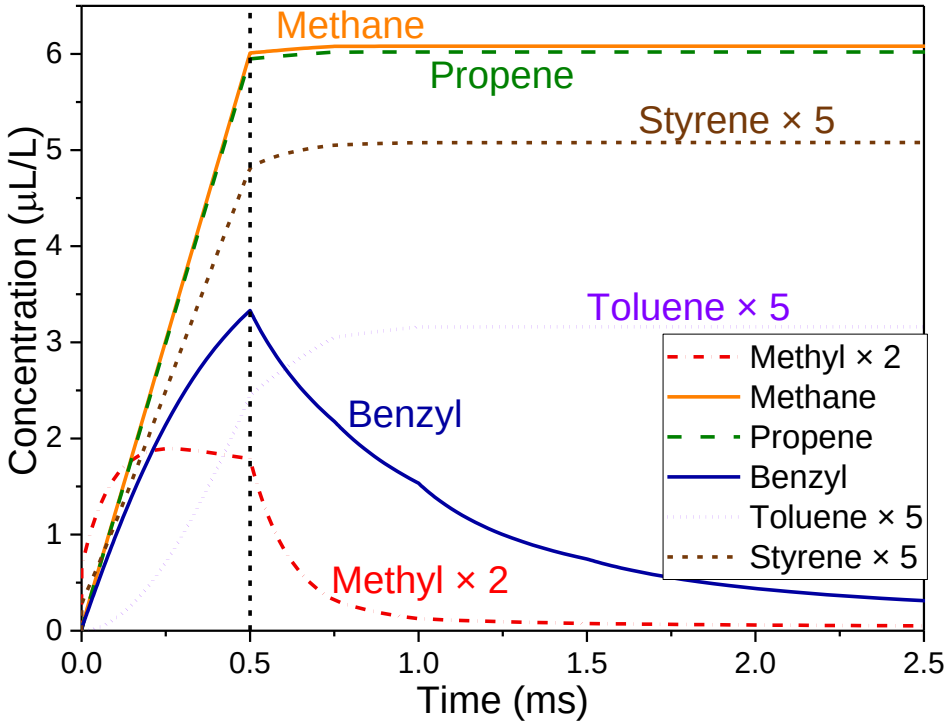

Figure 4. Time profiles (mixture B, 1041 K) for propene (green), methane (orange), toluene multiplied by five (purple), styrene multiplied by 5 (brown), benzyl radical (blue), and CH_3 (red) predicted by the kinetics model for chemistry during (0 ms to 0.5 ms) and after the shock (0.5 ms to 2.5 ms).

The first assumption that we make is that the main products are formed during the shock, and post-shock cooling is rapid (as noted above, we approximate this cooling with a stepwise function). Figure 4 shows the calculated time profiles of the species during and after a shock at 1041 K for mixture B. During the shock, propene increases linearly with time, as isopentylbenzene decomposes. After the shock, the propene concentration is constant, with 99 % already formed during the shock. Although not shown in the Figure 4, isobutene formation has nearly the same time dependence as propene. A similar trend is seen with styrene, and 94 % (typically 99 % or more at temperatures above 1100 K) or more of styrene is formed during the shock. A larger portion of styrene compared to propene is produced post-shock because a larger percentage of styrene is formed from radical attack.

While decomposition reactions will be quenched quickly after the shock, some radicals produced in the shock, especially CH_3 and benzyl radicals, will react post-shock. About 99 % of CH_3 radicals are formed during the shock (most from reaction R1a), but (5 to 20) % of these methyl radicals will react post-shock, with the largest percentage of post-shock chemistry occurring at low shock temperatures. While 99 % of the benzyl radicals are produced during the shock, (20 to 80) % will react post-shock. A significant proportion of the aromatic compounds we detect are formed post-shock; for example, about (10 to 50) % of EDMB is predicted to be formed post-shock from R1510. We expect larger uncertainties in the kinetics model prediction of the aromatic compounds that react post-shock, like toluene, ethylbenzene and EDMB.

We also assumed that most isobutyl radicals formed would decompose and not recombine with other radicals in the system, for example via the following reactions:

$$\text{benzyl} + \text{isobutyl} \rightarrow \text{isopentylbenzene} \qquad \text{(R1509)}$$

$$\text{3,5-dimethylbenzyl} + \text{isobutyl} \rightarrow \text{3,5-dimethyl-isopentylbenzene} \qquad \text{(R1515)}$$

Even with the above reactions included, the kinetics model predicts that 99.9 % of isobutyl loss is from the β-scission reactions (R1a and R1b + R1c). This agrees with the low concentration of isopentane from R1517 detected in our experiment and our assumption that isobutyl recombination was unimportant. A full reaction path analysis is shown in the supporting information, including the percentage of each compound predicted to be formed post-shock.

The sensitives of the ratio of [isobutene]/[propene] for both our model and the original JetSurF model for Mixture C at 1045 K and 1226 K are shown in Figure 5. This ratio would be directly equivalent to $(k_{1b} + k_{1c})/k_{1a}$ if no corrections for side chemistry were needed. For JetSurF, this ratio is about five times more sensitive to the reactions of interest, β-scission of the C-C or C-H bond (R1a and R1b + R1c), than any other reaction. The second most influential reaction is the decomposition of isopentylbenzene to make isobutyl radicals, which dominates radical production in the shock tube. Next in importance are the decomposition of isopentylbenzene to make isopropyl (R2b) and the abstraction of the tertiary hydrogen of isopentylbenzene by CH_3 (R3c), the main sources of propene and isobutene, respectively, from side chemistry. In our model the [isobutene]/[propene] ratio is less sensitive to the reactions of interest (R1a and R1b + R1c) than in JetSurF, because the secondary paths to isobutene are comparatively more important when (R1b + R1c) is slow relative to R1a. Propene formation is dominated by R1a in both models, but secondary chemistry, notably reactions of H and CH_3 with isopentylbenzene, has more influence as it becomes an important source of isobutene. Mixtures A and B, which have smaller inhibitor to isopentylbenzene ratios, show larger sensitivities to the side chemistry than seen in Figure 5, a result that confirms that the most reliable measurements are expected with Mixture C.

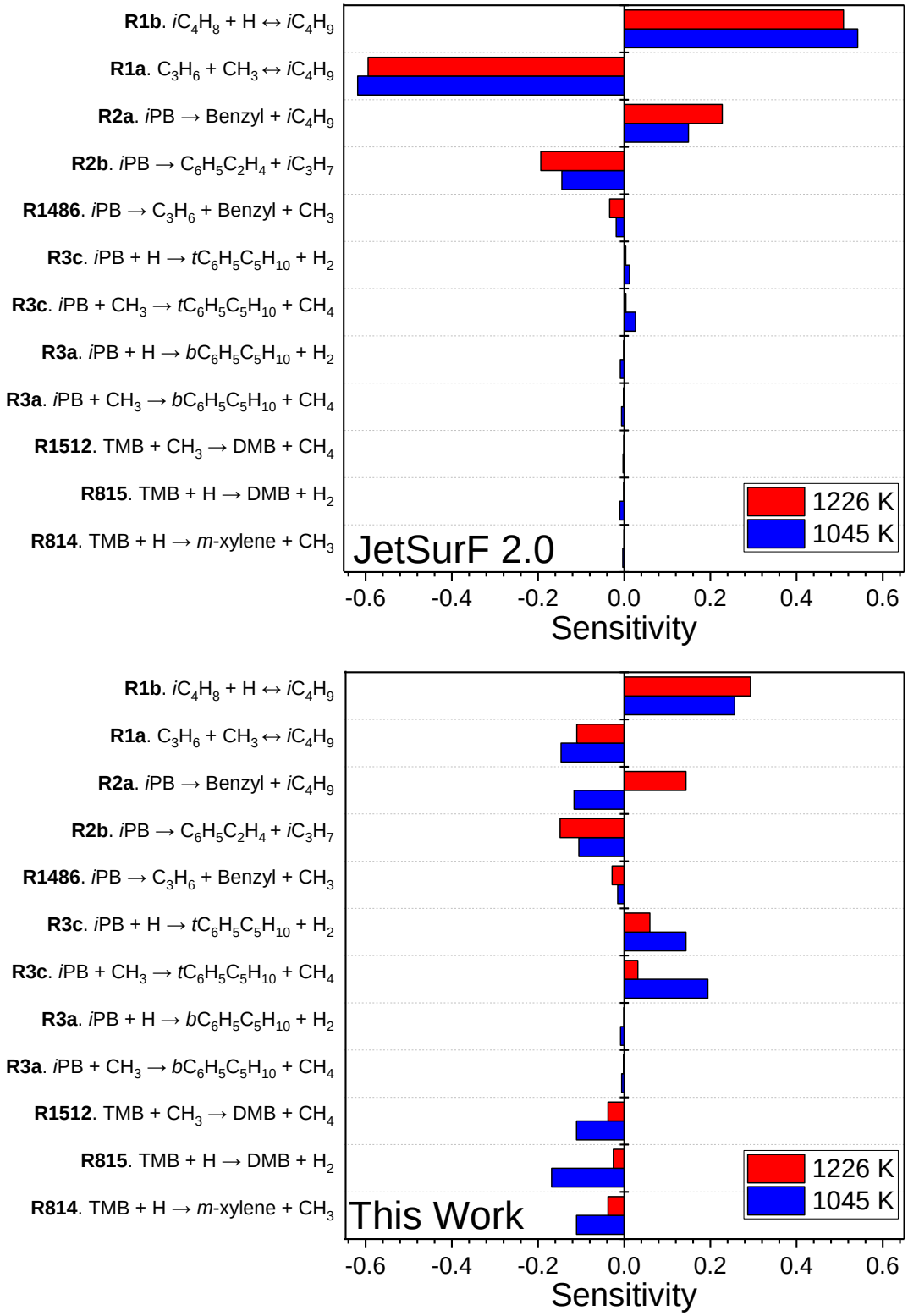

Figure 5. Sensitivity of JetSurF 2.0 (unmodified, top) and our kinetics model (bottom) prediction of [isobutene]/[propene] to key rate constants for mixture C at 1226 K (red) and 1045 K (blue). *i*PB = isopentylbenzene, TMB = 1,3,5-trimethylbenzene, DMB = 3,5-dimethylbenzyl

The concentrations of styrene and benzene will also affect our results, because they are used to correct for propene-producing side chemistry (E6). Figure 6 shows the sensitivity of the styrene and benzene concentration to different rate constants in our kinetics model. Styrene is most sensitive to reaction R2b, its main source under most experimental conditions. It is also sensitive to the branching ratio of 2-phenylethyl decomposition, R1500 and R1499, and mildly sensitive to H and CH_3 chemistry, including R3a and R3d. Similar sensitivities are seen for benzene, with is also primarily sensitive to R2b, R1500 and R1499. The kinetics model predicts, for most conditions, over 99 % of styrene and benzene formed have propene as a coproduct. At low temperatures, some benzene is formed from R3e (H substitution with isopentylbenzene), but this is at most 4 % of total benzene concentration. Minor decomposition of isopentylbenzene through fission of a methyl C-C bond leads to a small source of propene that does not have either styrene or benzene as a co-product:

$$\text{isopentylbenzene} \rightarrow CH_3 + C_3H_6 + \text{benzyl} \qquad \text{(R1486)}$$

This rate is easily estimated with analogy to the decomposition of isobutane,[46] and is at most 3.5 % of the total propene concentration and 15 % of the propene from side chemistry. This reaction typically introduces a (2 to 4) % error in $(k_{1b} + k_{1c})/k_{1a}$.

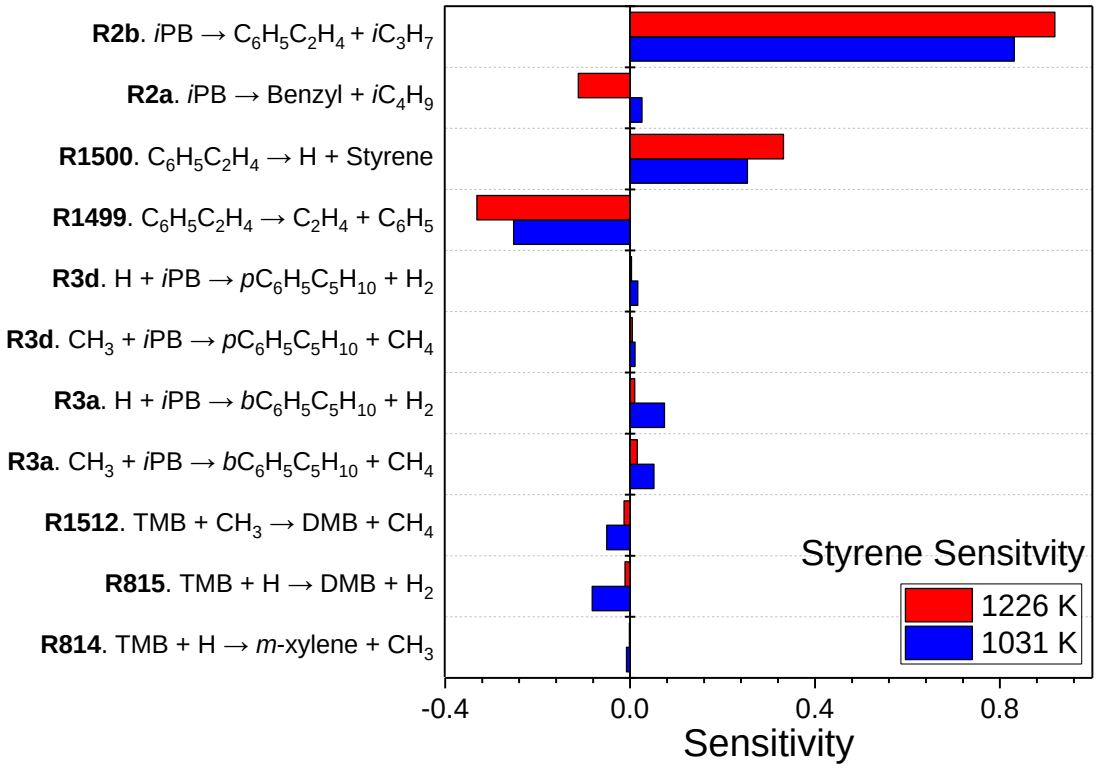

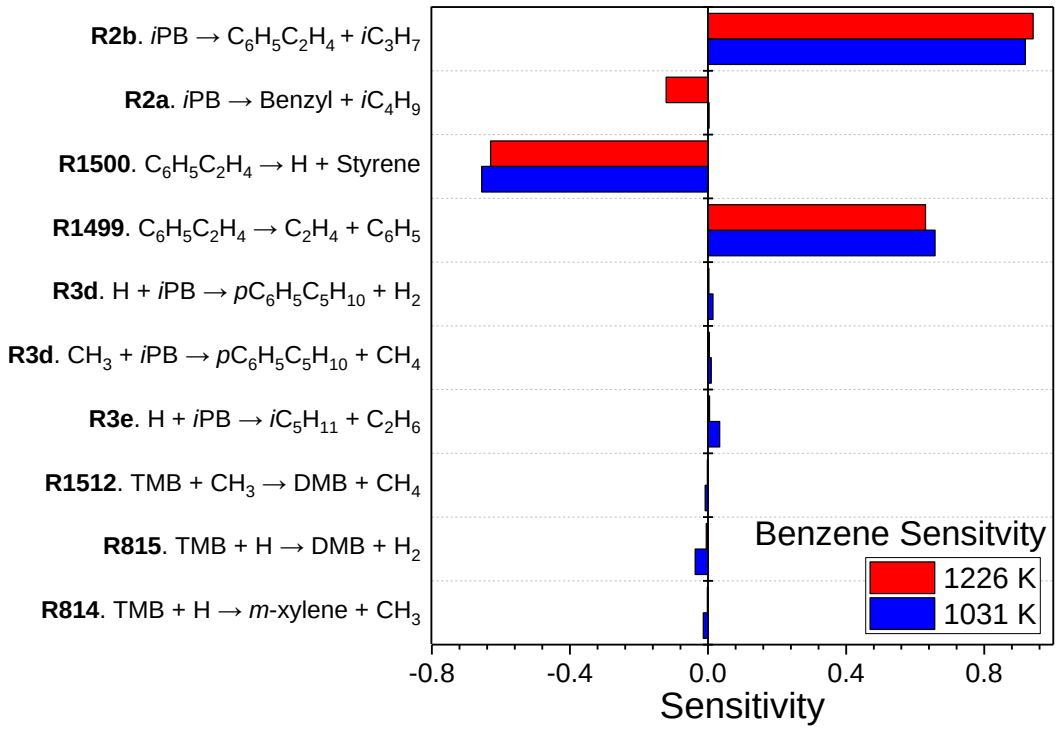

Figure 6. Sensitivity of the model prediction (kinetics model from this work) of styrene (top panel) and benzene (bottom panel) for mixture C at 1226 K and 1045 K. *i*PB = isopentylbenzene, TMB = 1,3,5-trimethylbenzene, DMB = 3,5-dimethylbenzyl.

When calculating the $(k_{1b} + k_{1c})/k_{1a}$ branching ratio (E6), the uncertainty in propene sources is dwarfed by uncertainties due to secondary production of isobutene. While the kinetics model predicts that the radical scavenger does work – over 95 % of H atoms will reaction with 1,3,5-trimethylbenzene – there is so little isobutene produced from the decomposition of isobutyl (R1b + R1c) that the isobutene concentration is easily perturbed by side chemistry. If there is an unaccounted-for secondary source of propene that is 1 % of the isobutyl concentration, the ratio will be too small by only 1 %; however, if there is an unknown source of secondary isobutene of the same amount, the ratio will be too large by 38 %. The model predicts isobutene produced from side chemistry is always at least 10 % of that produced by R1b + R1c, and typically more, leading to errors between 10 % (highest temperatures for all mixtures) and 800 % (at 959 K, mixture B) in $(k_{1b} + k_{1c})/k_{1a}$. This is much larger than any systematic error from secondary propene and is the reason why we interpret the branching ratio from equation E6, (2.5 ± 0.1) %, as the upper limit. The true value could still be significantly smaller, especially if we are not considering all side chemistry.

Predicted species concentrations from the kinetics models – our model, JetSurf 2.0,[6] AramcoMech 2.0[12] and LLNL[14-15] – are compared to measured values for selected shocks in Table 7. Our kinetics model predicts the absolute concentrations of most products to within a factor of 2. Propene was closely reproduced by our model, typically to within 10 % except at our lowest temperatures where minimal amounts of reaction R2a made quantitation more difficult and deviations were up to 30 %. The modeled sum of the main compounds from methyl chemistry (methane, ethane, ethylbenzene, and EDMB) was always within 46 % of the measured sum, and is typically within (20 to 30) %. This indicates accurate rate constants for isopentylbenzene decomposition, the main radical source. For all other compounds, there is

agreement well within an order of magnitude and usually well within a factor of two, even for aromatics formed post-shock. The exception is toluene, which we underpredict by over a factor of two. Since toluene is primarily from benzyl radicals, which are predicted to react significantly (typically 10 to 30 %) post-shock, quantification with the kinetics model is difficult.

Table 7. Comparison of model predictions[6, 12-13, 15] to measured concentrations for mixture C (1170 K and 363 kPa) and mixture A 1191 K, 274 kPa). All concentrations in μL/L (ppm).

	Measured	Model this work	Model JetSurF[6]	Model Aramco[12]	Model LLNL aromatics[15]	Model LLNL isooctane[13]
			Mixture C, 1170 K, 350 kPa			
Methane	23.0	14.5	11.6	13.2	13.5	13.0
Ethane	0.381	0.134	0.266	0.412	0.401	0.372
Ethylbenzene	1.35	1.86	2.01	1.69	1.54	1.48
EDMB	3.60	3.69	3.53	3.37	3.17	3.08
Propene	20.9	19.4	16.6	17.4	19.3	18.3
isobutene	0.432	0.411	3.08	2.33	0.560	1.51
Benzene	1.47	1.11	1.11	1.11	0.0283	0.0291
Toluene	8.82	4.37	4.39	4.40	4.00	4.01
m-Xylene	4.87	4.26	4.30	4.89	3.04	3.28
Styrene	2.06	2.21	2.20	2.21	3.30	3.31
CH_3 Budget*	28.7	20.3	17.6	19.0	19.0	18.3
			Mixture A, 1191 K, 274 kPa			
Methane	61.4	25.0	16.8	18.9	22.1	21.1
Ethane	9.96	3.42	5.38	8.45	10.5	9.66
Ethylbenzene	32.1	35.8	31.9	28.5	26.5	25.4
EDMB	29.5	24.8	23.0	20.4	21.1	21.1
Propene	127	100.	86.9	88.8	100.	95.4
isobutene	3.26	3.02	16.1	14.4	3.65	8.53
Benzene	3.31	6.17	6.26	6.32	0.396	0.428
Toluene	20.9	4.86	5.11	5.25	4.37	4.47
m-Xylene	13.8	11.1	14.1	14.4	9.30	10.4
Styrene	13.1	12.9	12.9	13.0	19.3	19.4
CH_3 Budget*	143	92.5	82.4	84.8	90.7	87.0

*CH_3 budget is the sum of all compounds that come from CH_3 radicals, or [Methane] + 2×[Ethane] + [Ethybenzene] + [EDMB]

Most of the literature kinetics models greatly overpredict isobutene concentration, indicating that the model values for the branching ratio, $(k_{1b} + k_{1c})/k_{1a}$ are too high. Both JetSurF

and AramcoMech 2.0 over predict isobutene by at least 300 % for all conditions (up to 500 % at low temperatures); LLNL isooctane overpredicts by (100 to 250) %. LLNL aromatics agrees with our experimental isobutane concentrations, almost always within 50 %. Since our model was modified to fit the data, it well predicts isobutene concentrations, almost always within 10 %. All models predict that propene will be the main product of isobutyl decomposition (branching ratio > 50 %), with propene concentrations predicted within 50 % of the experiment for all conditions.

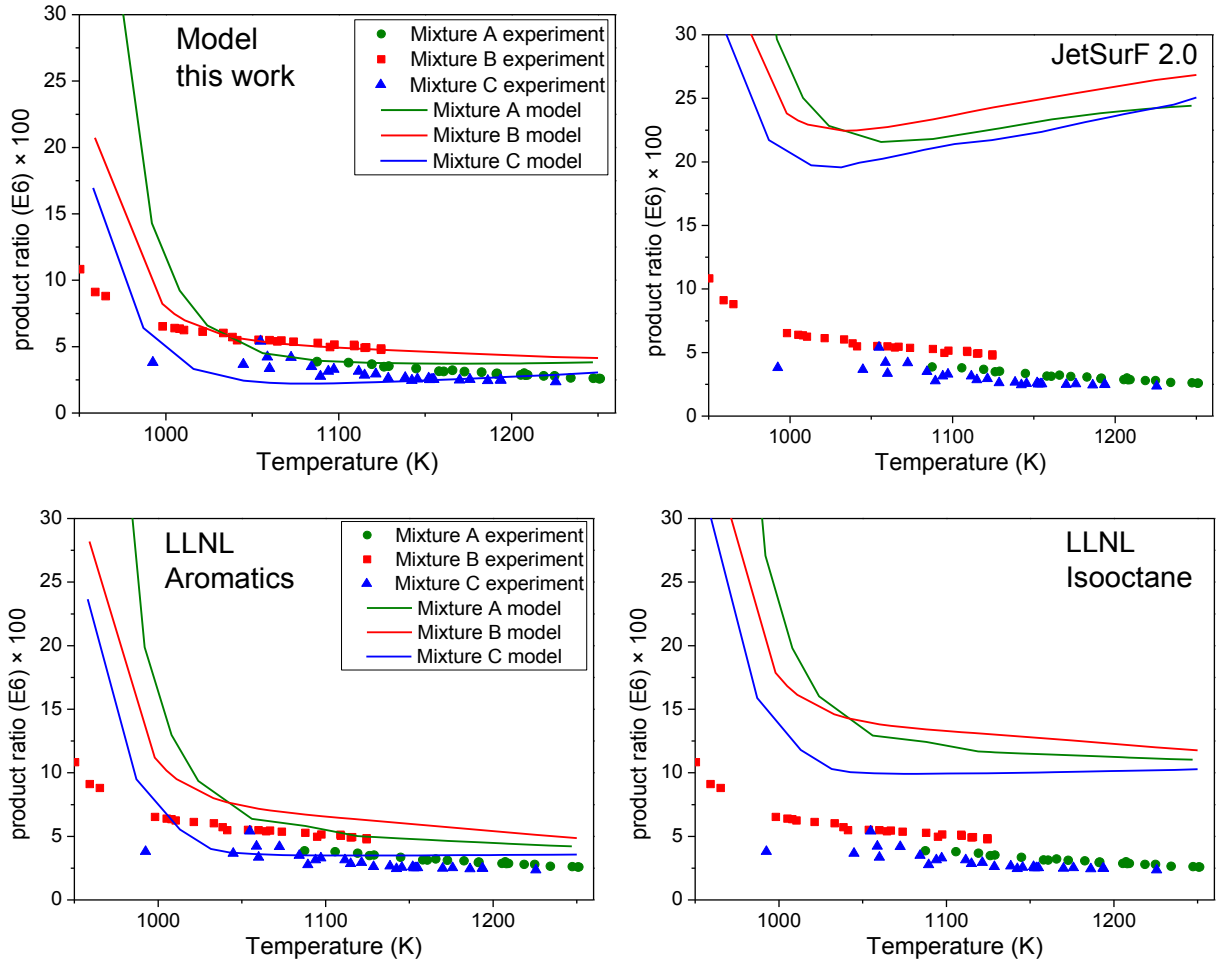

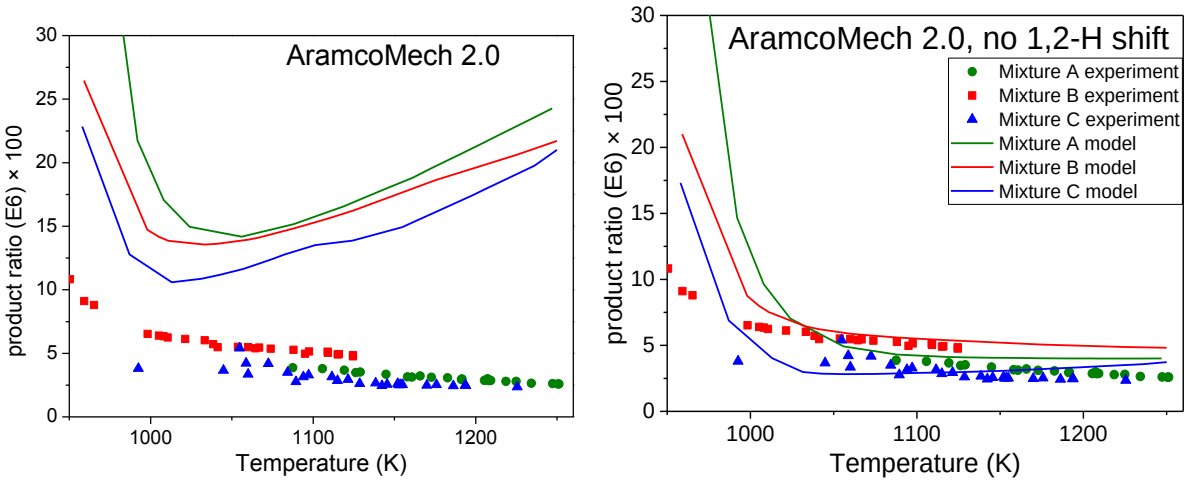

Figure 7. The ratio of isobutene to corrected propene (equation E6) as a function of temperature for all mixtures compared to the kinetics model from this work, JetSurF 2.0, LLNL aromatics, LLNL isooctane and AramcoMech 2.0. Model predictions are calculated from predicted product concentrations, not from $(k_{1b} + k_{1c})/k_{1a}$, so the model values include side chemistry. We also include model predictions for AramcoMech 2.0 after we removed their R1c from the mechanism, leaving only R1a and R1b; this will be discussed later (Sections 5 and 6).

Predictions for the ratio of isobutene to corrected propene (equation E6) for our model, JetSurF,[6] AramcoMech[12] and LLNL[14-15] are compared to the experimental data in Figure 7. Our model and LLNL aromatics have generally good agreement with the experimental data as well as the same qualitative temperature dependence (isobutene decreases relative to corrected propene with temperature, especially at temperatures < 1000 K). Both these models capture the decrease in ratio with radical concentration. LLNL isooctane predicts a similar temperature and radical scavenger concentration dependence as LLNL aromatics, but with more than double the ratio at high temperatures. For AramcoMech 2.0 and JetSurF, the model disagrees both quantitatively and qualitatively with the experiment, predicting high ratios that increase with temperature. At temperatures above 1250 K, these models could even more dramatically overpredict the branching ratio of isobutene.

Our model predicts that $(k_{1b} + k_{1c})/k_{1a}$ is determined well from our experimental results and equation E6. The calculated branching ratio is predicted to be different from the actual value

by only 15 % at 1100 K and 5 % at 1225 K for mixture C. Most of this discrepancy is from secondary isobutene (R3c) formation, with propene from side chemistry unaccounted for by benzene and styrene leading to a discrepancy of only (2 to 4) %. If the kinetics model well-characterizes our system, side chemistry does not greatly affect the experimental value of Mixture C for $(k_{1b} + k_{1c})/k_{1a}$ presented in section 3.3 of (2.5 ± 0.1) % (2σ, from experimental scatter). Our kinetics model predicts that this value should be (2.5 ± 0.4) % including side chemistry (2σ, error is standard deviation in the model's predicted value for all experiments of mixture C above 1100 K). When only considering propene and isobutene from R1, the model predicts this ratio should be (2.3 ± 0.5) %. To get a conservative upper limit, we take our experimental value of 2.5 %, but combine the errors from the kinetics model and experimental scatter, leading to a value of (2.5 ± 0.5) %.

5. DISCUSSION

Under our conditions we detect a low level of C-H bond scission in the isobutyl radical, with an apparent measured value of (2.5 ± 0.5) % and a well-defined maximum value of 3.0 %. This is a kinetic result. It is consistent with the thermodynamics of beta scissions in alkyl radicals, wherein bond dissociation energies (BDEs) of C-C bonds are well-known to be smaller than those of the corresponding C-H bonds. Bond strength differences are typically (32 to 40) kJ/mol, a result easily determined from experimental, theoretical, or group-additivity derived thermodynamic values.[69-75] The computed ΔBDE in the isobutyl case is 32.7 kJ/mol.[75] The relative kinetics of C-H and C-C beta scissions differ, however, from the thermodynamic BDE differences due to differing intrinsic barrier heights for the reverse additions of H atoms and alkyl radicals, as well as differences in the transition state entropies. Even relatively small

uncertainties in these properties can impact the derived beta scission ratios, which is part of the reason why significantly different branching values appear in the models.

Because our experimental result does not distinguish between R1b and R1c, our data require that, in addition to minimal direct C-H β-scission, there is little or no 1,2-shift reaction in isobutyl radicals. While other H-shift isomerization reactions are known to happen in the gas phase, 1,2 H shifts are unfavorable, a result that has been interpreted in terms of ring strain in the transition state.[76] In his 2007 review, Poutsma[76] evaluated previous experimental and theoretical work on 1,*x* H-shifts and estimated relative ring stain energies of (27.5, 26.5, 6.2 and 0.0) kJ/mol for 1,2; 1,3; 1,4; and 1,5 H-shifts, respectively. Hayes and Burgess[20] in 2009 suggested that 1,2 H-shifts are fundamentally different from other 1,*x* H-shifts and are not "internal abstractions" but "atom migrations" with slightly lower activation barriers than 1,3 H-shifts.[20, 77] Their calculated barrier for a 1,2 H-shift from a primary radical to a tertiary radical is 152 kJ/mol, which they conclude is high but not high enough to exclude the possibility in small hydrocarbons.[20] Davis and Francisco[77] in 2011 calculated the high-pressure theoretical rate constants (including tunneling transmission coefficients) for hydrogen-shift isomerizations in *n*-alkyl radicals, and found that near 1000 K, 1,2-H shifts are typically four orders of magnitude slower than 1,5-H shifts. However, the isomerization barriers scale with the exothermicity, so the primary to tertiary conversion (like the 1,2 H-shift in isobutyl radicals) is expected to be the most favorable.[28, 32] Wang *et al.*[28] reported in 2015 quantum and transition-state theory calculations of the high-pressure rate constants for a large number of 1,2-H shifts, and found that the 1,2-H shift in isobutyl, which involves a favorable conversion from a primary to tertiary radical, was approximately an order of magnitude faster than for *n*-alkyl radicals. Even at infinite pressures

and temperatures up to 2000 K, this reaction was still at least an order of magnitude smaller than C-C β-scission rate constants.[28]

Table 8. Threshold Energies (in kJ/mol) for unimolecular reactions of isobutyl radicals.

Reaction	Threshold Energy (E_0)*	Source
C-C β-scission	122	Yamauchi *et al*. estimated for generic primary alkyl radical[23]
C-H β-scission	143	Yamauchi *et al*. for estimated generic primary alkyl radical[23]
1,2 H-shift	152	Hayes and Burgess[20]

Our best estimates for the threshold energy (the amount of energy needed for reaction to take place, including the kinetic energy of the gas) for each of the competing reactions of interest are listed in Table 8. These should be comparable to experimental activation energies of R1a, R1b, and R1c and suggest that the relative amount of C-H β-scission should increase with temperature if all rate constants are at their high-pressure limits (i.e. the reacting molecules have a Boltzmann energy distribution). Barker and Ortiz[67] describe that when a molecule has more than one unimolecular reaction, the reaction with the lowest activation energy will deplete the populations in the higher energy states more rapidly than if there were a single reaction channel having the higher activation energy; falloff for high activation energy channels is thus increased in multichannel systems. In the pressure dependent region, the rate of C-H β-scission and 1,2-H-shift should be lower than expected based solely on their activation energies due to this population depletion. Studying the unimolecular reactions of 2-methylhexyl radicals with RRKM theory, Barker and Ortiz[67] found that this effect was small, but present, at pressures of about 100 kPa, close to the conditions of our experiment. The effect should increase with temperature as the reaction moves further into the fall-off region. In our experiments, however, there is an offsetting increase in the shock pressure that occurs with increasing shock temperature, so that

the net result is uncertain. Figure 3 shows $(k_{1b} + k_{1c})/k_{1a}$ decreases with temperature and pressure – the opposite of what we would expect from the high pressure limiting ratio of C-H to C-C β-scission. While some of this could be due to the population depletion effect, the very rapid increase in the [isobutene]/[propene] branching ratio at low temperatures is more consistent with side chemistry.

Experimental investigations on the branching in the decomposition of isobutyl and other alkyl radicals have historically shown a high degree of variation. Much of the early literature on isobutyl and propyl decomposition focused on the possibility of 1,2-H-shifts, with studies giving a large range of values for the activation energy, ranging from 123 kJ/mol[22] to 168 kJ/mol.[9] In 1958, Heller and Gordon[21] studied the decomposition of isopropyl-d_1 radicals and estimated that approximately 50 % of the isopropyl radicals underwent 1,2 H-shifts. This was contradicted by later work from Kerr and Trotman-Dickenson,[22] who found a branching ratio of C-H to C-C β-scission for isopropyl radicals of up to 25 % based on anomalous ethene and methane formation. As with our data, they found that this ratio decreased when the temperature increased (293 to 774) K, a result that disagrees with current theoretical knowledge and suggests perturbation by side chemistry. In a series of papers from the 1960s on strategically-deuterated, isopropyl and isobutyl radicals, Jackson and McNesby[8-10] set upper limits on the amount of 1,2 H-shifts and C-H β-scission at (472 to 813) K of 7 % for isopropyl and 1 % for isobutyl and argued that these upper limits were lower than other literature values because their experiments were free from nonthermal photochemistry.[9] Multiple other researchers claimed significant 1,2 H-shift branching ratios for decades afterwards.[24-26, 78-79] These claims were usually based, however, on the detection of compounds that could easily be produced from side chemistry, including methane and ethene.[24-25]

More recent experimental work by Yamauchi *et al*.[23] in 1999 provides strong evidence against 1,2 H-shifts and competitive C-H β-scissions. At (900 to 1400) K and about 100 kPa, they photolyzed a series of alkyl iodides to make alkyl radicals (including isopropyl, *n*-propyl, *n*-butyl, *s*-butyl and isobutyl), detected iodine atoms to quantify the initial of alkyl radical concentration, and detected H atoms to quantify how much of the alkyl radical underwent C-H β-scission or 1,2 H-shifts. For radicals like isopropyl which have no CH_3 group β to the radical, they found H concentration approximately equal to the initial alkyl radical concentration, denoting that every radical undergoes C-H β-scission with no significant isomerization. For compounds like isobutyl which could undergo C-C or C-H bond scission, they detected almost no H atoms – a little over 3 % for isobutyl radicals, a value in close agreement with the present work, indicating little or no C-H β-scission. Yamauchi *et al.* noted that the amount of H detected correlated inversely with the purity of the alkyl iodide precursor and that even this 3 % H atom yield is potentially explainable by side chemistry.

In our experiments, there was also an increase in the products expected from C-H β-scission under conditions conducive to side chemistry: lower temperatures and lower amounts of radical scavenger. If significant amounts of C-H scission or 1,2 H-shifts did occur, all experiments reported in the literature should have detected the products. However, the branching fraction of products from C-H β-scission (or 1,2 H-shifts) varies greatly between research groups and is correlated with side chemistry. There are now several high quality experimental results,[8, 10, 23] including this work, that show no evidence for significant amounts of either C-H β-scission or 1,2 H-shifts in isobutyl radicals. We conclude that these reactions are at most a very minor channel.

While there are examples of experimental, [7, 29-30, 80] theoretical[81-82] and modeling[15] work that assume little or no C-H scission or 1,2 H-shifts, many commonly used kinetics models for combustion still assume much larger amounts of H atoms from the decomposition of alkyl radicals than is suggested by the present data, other high-quality experiments, and recent theoretical studies. Figure 8 shows values used in the literature for the relative rates of C-H β scission and C-C β-scission of isobutyl and selected alkyl radicals. To better compare the data, the branching values in Figure 8 have been scaled to the number of H and alkyl leaving groups; that said, such scaling ignores potentially important differences in the relative thermochemistry and should be treated as a first-order approximation.

Figure 8 shows that some of the ratios used in the literature are more than an order of magnitude higher than our experimental results. JetSurF 2.0[6] predicts the two pathways being approximately equal at high pressures, having a ratio of about (20 to 60) %. This branching ratio decreases to (10 to 25) % at 101.3 kPa and is significantly higher than the JetSurF 2.0 value for the decomposition of *n*-propyl, which has a branching ratio of below 10 % even at the high-pressure limit. This is inconsistent, since we believe that this ratio should be higher for *n*-propyl radicals due to differences in the thermochemistry.

While AramacoMech 2.0 is within our upper limit at 800 K and 101.3 kPa, its branching ratio quickly increases to above 100 % by 1300 K. AramcoMech 2.0 is the only model where the branching ratio decreases with pressure, leading to a higher branching ratio at 101.3 kPa than at infinite pressure. As shown in Table 1, their rate constants for isobutyl C-C and C-H bond scission (R1a and R1b) included fall-off behavior while the rate constant for isobutyl isomerization (R1c) did not. Their high-pressure limit for R1c is from Matheu *et al*.[32] and is reasonably consistent with the 2015 value of Wang *et al*.,[28] but it is not applicable to pressures

near 100 kPa. This effect will become even more pronounced at lower pressures, with AramcoMech 2.0 predicting near all 1,2 H-shift isomerization and no R1a at 10.1 kPa and temperatures above 1200 K. As was shown in Figure 7, simply removing R1c from their model leads to good agreement with our data.

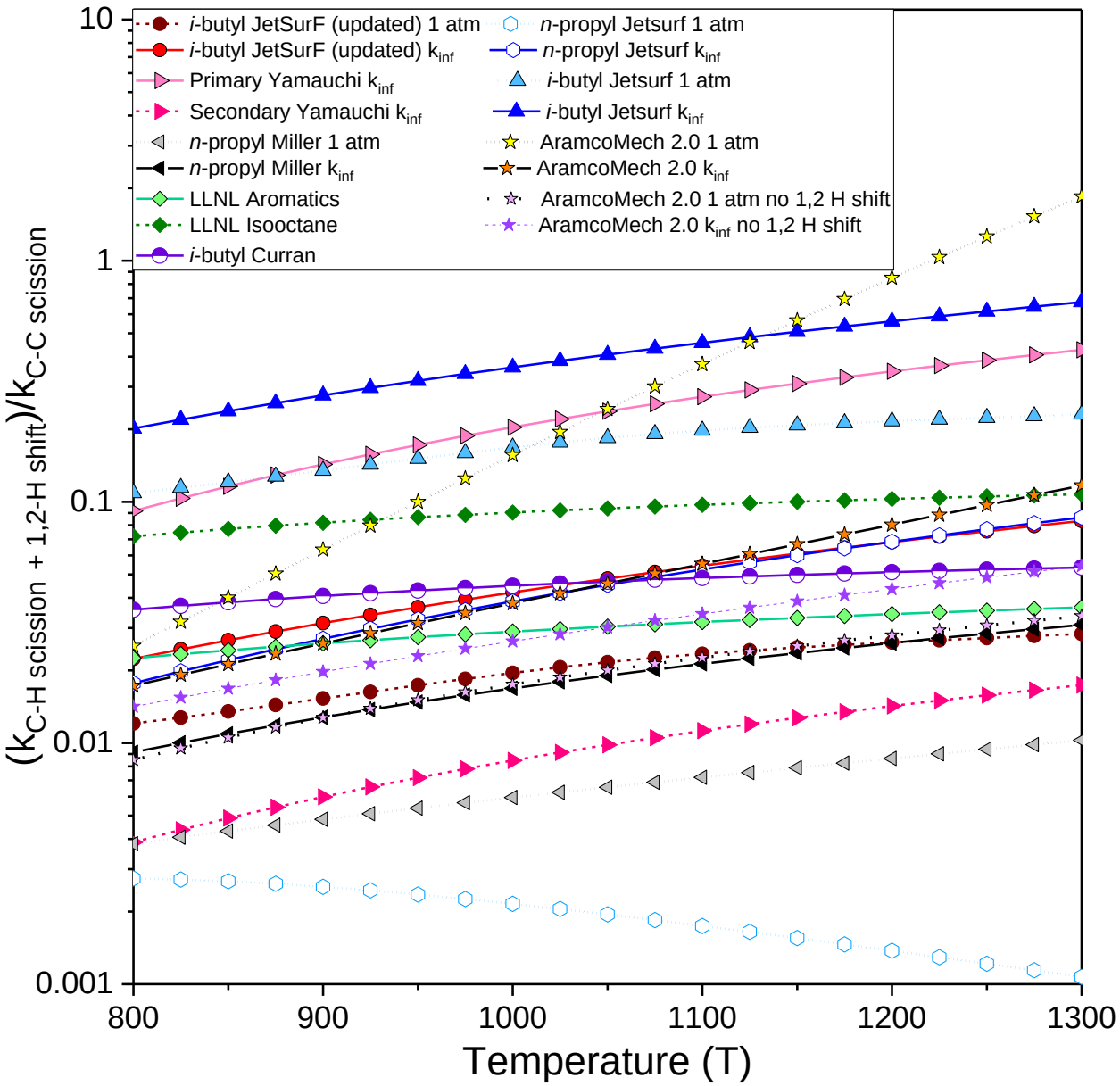

Figure 8. Relative rates of C-H and C-C β-scission from the literature[1, 23, 33] and used in kinetics models.[6, 12-13, 15-16, 29-30] Branching ratios for compounds other than isobutyl have been scaled for the number of H and CH_3 as to be directly comparable to isobutyl.

The LLNL isooctane model,[13] which uses rate constants estimated based on the reverse process as described by Curran *et al*. in 1998,[18] gives pressure-independent C-H branching values of (7 to 10) % from (800 to 1300) K. These ratios are significantly lower than JetSurF or AramcoMech 2.0, but are still significantly higher than our suggested value. Their modeled ratio exhibits only mild temperature dependence and will remain at or below 12 % for temperatures up to 3000 K. The rate constant is given without pressure dependence, meaning that its branching ratio will be (5 to 12) % for all pressures and temperatures from (600 to 3000) K. However, modelers should be cautious if their system contains significant amounts of isobutyl decomposition, because this (5 to 12) % would create highly-reactive H atoms, starting radical chain chemistry.

LLNL aromatics[15] is the only literature model explored whose branching ratio is below our upper limit for all temperatures (800 to 1300) K. Like LLNL isooctane, its branching ratio is not pressure dependent. If the pressure is significantly increased from the conditions of our experiments, (200 to 400) kPa, there could be more C-H β-scission; however, their pressure-independent rate constants should work for most systems. The LLNL biodiesel's branching ratio (Table 1, not shown on Figure 7 or Figure 8) is between those of LLNL isooctane and LLNL aromatics, again with no pressure dependence.

6. RECOMMENDED RATE CONSTANTS

The above analysis suggests the need for selected amendments to current kinetics models to better reflect the available high-quality literature data on the relative favorability of C-C and C-H β-scission. A full theoretical treatment of the isobutyl system has not been undertaken to our knowledge and, at present, there exist no benchmark experimental data on the branching ratio at temperatures above ~1300 K or spanning a wide pressure range; such data would better define

the fall-off behavior and test RRKM predictions. The most complete analysis of a related well-characterized system is from Miller and Klippenstein,[33] who used high level theory validated by comparison with experiment to derive pressure and temperature dependent rate constants for the decomposition of *n*-propyl radicals. While some differences between isobutyl and *n*-propyl will arise from differences in the reaction energetics, the change in the number of H and CH_3 leaving groups, and changes in the fall-off behavior due to the molecular size difference, these calculations are a reasonable starting point for estimates. In AramcoMech 2.0, the rate constant for R1b is based on Miller and Klippenstein,[33] while the value for R1a is indicated as an estimate from "K. Zhang" (as commented in the model). The basis of the latter is not documented. Nonetheless, the resulting estimate of the branching ratio is consistent with our data and upper limit; it also gives estimates that are similar to those of our updated JetSurF model. Importantly, both our updated JetSurF model and the AramcoMech 2.0 model include parameterization intended to approximate the pressure dependent behavior. Both describe the available data within the current uncertainties. We recommend these values until a more complete analysis is available, with the caveat that there remain questions – and essentially no data – regarding the behavior at high pressures, particularly at temperatures above 1300 K. Note that the AramcoMech 2.0 rate constant for R1c should be removed to avoid significant overproduction of H atoms via the 1,2-H shift isomerization.

If other parameterizations are chosen, we encourage modelers to ensure that their rates have a branching ratio of C-H β-scission to C-C β-scission ($(k_{1b} + k_{1c})/k_{1a}$) of no more than 3.0 % at temperatures and pressures less than 1250 K and 400 kPa, respectively. Because 1,2 H shift processes are inherently included in our recommended maximum, the sum of the direct and indirect paths should be considered when rate constants are selected.

7. CONCLUSIONS

We place an upper limit of 3.0 % for the branching ratio of H in the decomposition of isobutyl radicals at (950 to 1250) K and (200 to 400) kPa using shock tube experiments. These data show that C-H β-scission and 1,2 H shift reactions are very minor compared with C-C β-scission. Our results are in agreement with the experiments of Yamauchi *et al*.[23] and Jackson and McNesby;[8-10] as well as theoretical calculations.[20, 28, 33] Comparisons show that some current kinetics models could be improved with lower branching ratios for C-H β-scission and 1,2 H shift reactions.

Finally, we think it important to applaud the on-going efforts of researchers within the combustion community - particularly those whose models we have used - to make their work readily available in a standard format. The present effort is one demonstration of how this can pave the way for community-based improvement and vetting.

ASSOCIATED CONTENT

Supporting Information is available free of charge.

Full table of all products detection in the shock tube experiments (.xlsx)

All Cantera kinetics model used in this work (.txt).

Reaction path analysis with percentage of key compounds formed post-shock (.pdf)

Isopentylbenzene decomposition rate constants from individual experiments (.xlsx)

AUTHOR INFORMATION

Corresponding Authors

(L.A.M.) E-mail: laura.mertens@nist.gov. Phone: 301-975-2077.

(J.A.M.) E-mail: jeffrey.manion@nist.gov. Phone: 301-975-3188.

Notes

The authors declare no competing financial interest.

Disclaimer: certain commercial materials and equipment are identified in this paper in order to specify adequately the experimental procedure. In no case does such identification imply recommendation of endorsement by the National Institute of Standards and Technology, nor does it imply that the material or equipment is necessarily the best available for the purpose.

ACKNOWLDGEMENTS

LAM would like to thank the National Academy of Science's NRC Research Associateship Program for financial support. We would like to thank Dave Sheen for technical support with the Cantera kinetics models and the MUM-PCE 0.1 software package.

REFERENCES

(1) Curran, H. J. Rate constant estimation for C-1 to C-4 alkyl and alkoxyl radical decomposition. *Int. J. Chem. Kinet.* **2006,** *38,* 250-275.

(2) Westbrook, C. K.; Dryer, F. L. Chemical kinetic modeling of hydrocarbon combustion. *Prog. Energy Combust. Sci.* **1984,** *10,* 1-57.

(3) Pilling, M. J. Reactions of hydrocarbon radicals and biradicals. *J. Phys. Chem. A* **2013,** *117,* 3697-3717.

(4) Pacansky, J.; Waltman, R. J.; Barnes, L. A. Studies on the structure and beta-bond scission reactions of primary alkyl radicals, $CH_3(CH_2)NCH_2$•, for n=1-6. *J. Phys. Chem.* **1993,** *97,* 10694-10701.

(5) Tsang, W. The stability of alkyl radicals. *J. Am. Chem. Soc.* **1985,** *107,* 2872-2880.

(6) Wang, H.; Dames, E.; Sirjean, B.; Sheen, D. A.; Tango, R.; Violi, A.; Lai, J. Y. W.; Egolfopoulos, F. N.; Davidson, D. F.; Hanson, R. K., et al. A high-temperature chemical kinetic model of n-alkane (up to n-dodecane), cyclohexane, and methyl-, ethyl-, n-propyl and n-butyl-cyclohexane oxidation at high temperatures, JetSurF version 2.0, http://web.stanford.edu/group/haiwanglab/JetSurF/JetSurF2.0/index.html (accessed Jan 9, 2017).

(7) Knyazev, V. D.; Slagle, I. R. Unimolecular decomposition of *n*-C4H9 and *iso*-C4H9 radicals. *J. Phys. Chem.* **1996,** *100,* 5318-5328.

(8) Jackson, W. M.; Darwent, B. D.; McNesby, J. R. Thermal reactions of isobutyl radicals. *J. Chem. Phys.* **1962,** *37,* 2256-2260.

(9) Jackson, W. M.; McNesby, J. R. Thermal isomerization of isopropyl-1,1,1-d_3 radicals. *J. Chem. Phys.* **1962,** *36,* 2272-2275.

(10) McNesby, J. R.; Jackson, W. M. On the isomerization of isobutyl radicals. *J. Chem. Phys.* **1963,** *38,* 692-693.

(11) Zhou, C.W.; Li, Y.; O'Connor, E.; Somers, K. P.; Thion, S.; Keesee, C.; Mathieu, O.; Petersen, E. L.; DeVerter, T. A.; Oehlschlaeger, M. A., et al. A comprehensive experimental and modeling study of isobutene oxidation. *Combust. Flame* **2016,** *167,* 353-379.
(12) Li, Y.; Zhou, C.-W.; Somers, K. P.; Zhang, K.; Curran, H. J. The oxidation of 2-butene: A high pressure ignition delay, kinetic modeling study and reactivity comparison with isobutene and 1-butene. *Proc. Combust. Inst.* **2017,** *36,* 403-411.
(13) Curran, H. J.; Gaffuri, P.; Pitz, W. J.; Westbrook, C. K. A comprehensive modeling study of iso-octane oxidation. *Combust. Flame* **2002,** *129,* 253-280.
(14) Herbinet, O.; Pitz, W. J.; Westbrook, C. K. Detailed chemical kinetic mechanism for the oxidation of biodiesel fuels blend surrogate. *Combust. Flame* **2010,** *157,* 893-908.
(15) Nakamura, H.; Darcy, D.; Mehl, M.; Tobin, C. J.; Metcalfe, W. K.; Pitz, W. J.; Westbrook, C. K.; Curran, H. J. An experimental and modeling study of shock tube and rapid compression machine ignition of n-butylbenzene/air mixtures. *Combust. Flame* **2014,** *161,* 49-64.
(16) Goos, E.; Hippler, H.; Hoyermann, K.; Jurges, B. Reactions of methyl radicals with isobutane at temperatures between 800 and 950 Kelvin. *Int. J. Chem. Kinet.* **2001,** *33,* 732-740.
(17) Mehl, M.; Pitz, W. J.; Westbrook, C. K.; Curran, H. J. Kinetic modeling of gasoline surrogate components and mixtures under engine conditions. *Proc. Combust. Inst.* **2011,** *33,* 193-200.
(18) Curran, H. J.; Gaffuri, P.; Pitz, W. J.; Westbrook, C. K. A comprehensive modeling study of n-heptane oxidation. *Combust. Flame* **1998,** *114,* 149-177.
(19) Metcalfe, W. K.; Burke S. M.; Ahmed S. S.; Curran H. J. A Hierarchical and Comparative Kinetic Modeling Study of $C_1 - C_2$ Hydrocarbon and Oxygenated Fuels. *Int. J. Chem. Kinet.* **2013,** *45,* 638-675.
(20) Hayes, C. J.; Burgess, D. R. Kinetic barriers of H-atom transfer reactions in alkyl, allylic, and oxoallylic radicals as calculated by composite *ab initio* methods. *J. Phys. Chem. A* **2009,** *113,* 2473-2482.
(21) Heller, C. A.; Gordon, A. S. Isopropyl radical reactions. 2. Photolysis of diisopropyl ketone-d_2. *J. Phys. Chem.* **1958,** *62,* 709-713.
(22) Kerr, J. A.; Trotman-Dickenson, A. F. The reactions of alkyl radicals. Part 2.-s-propyl radicals from the photolysis of isobutyraldehyde. *Trans. Faraday Soc.* **1959,** *55,* 921-928.
(23) Yamauchi, N.; Miyoshi, A.; Kosaka, K.; Koshi, M.; Matsui, N. Thermal decomposition and isomerization processes of alkyl radicals. *J. Phys. Chem. A* **1999,** *103,* 2723-2733.
(24) Szirovicza, I.; Márta, F. Thermal isomerization of isopropyl radicals. *React. Kinet. Catal. Lett.* **1975,** *3,* 155-160.
(25) Szirovicza, L.; Márta, F. Some reactions of isopropyl radicals. *Int. J. Chem. Kinet.* **1976,** *8,* 897-910.
(26) Gordon, A. S.; Tardy, D. C.; Ireton, R. Ethyl radical isomerization - 1,2-hydrogen (deuterium) shifts in pyrolysis of 1,1,1-trideuterioethane. *J. Phys. Chem.* **1976,** *80,* 1400-1404.
(27) Szirovicza, L.; Szilagyi, I. Thermal-decomposition of 2,2-propane-d_2. CH_3CDCH_3 radical isomerization. *Int. J. Chem. Kinet.* **1980,** *12,* 113-122.

(28) Wang, K.; Villano, S. M.; Dean, A. M. Reactivity–structure-based rate estimation rules for alkyl radical H atom shift and alkenyl radical cycloaddition reactions. *J. Phys. Chem. A* **2015,** *119,* 7205-7221.
(29) Manion, J. A.; Sheen, D. A.; Awan, I. A. Evaluated kinetics of the reactions of H and CH_3 with n-alkanes: experiments with n-butane and a combustion model reaction network analysis. *J. Phys. Chem. A* **2015,** *119,* 7637-7658.
(30) Comandini, A.; Awan, I. A.; Manion, J. A. Thermal decomposition of 1-pentyl radicals at high pressures and temperatures. *Chem. Phys. Lett.* **2012,** *552,* 20-26.
(31) Tsang, W. Chemical kinetic data base for combustion chemistry part V. propene. *J. Phys. Chem. Ref. Data* **1991,** *20,* 221-273.
(32) Matheu, D. M.; Green, W. H.; Grenda, J. M. Capturing pressure-dependence in automated mechanism generation: Reactions through cycloalkyl intermediates. *Int. J. Chem. Kinet.* **2003,** *35,* 95-119.
(33) Miller, J. A.; Klippenstein, S. J. Dissociation of propyl radicals and other reactions on a C_3H_7 potential. *J. Phys. Chem. A* **2013,** *117,* 2718-2727.
(34) Manion, J. A.; McGivern, W. S. The importance of relative reaction rates in the optimization of detailed kinetic models. *Int. J. Chem. Kinet.* **2016,** *48,* 358-366.
(35) Manion, J. A.; Awan, I. A. The decomposition of 2-pentyl and 3-pentyl radicals. *Proc. Combust. Inst.* **2013,** *34,* 537-545.
(36) Manion, J. A.; Awan, I. A. Evaluated kinetics of terminal and non-terminal addition of hydrogen atoms to 1-alkenes: A shock tube study of H + 1-butene. *J. Phys. Chem. A* **2015,** *119,* 429-441.
(37) Manion, J. A.; Sheen, D. A.; Awan, I. A. Evaluated kinetics of the reactions of H and CH_3 with n-alkanes: Experiments with n-butane and a combustion model reaction network analysis. *J. Phys. Chem. A* **2015,** *119,* 7637-7658.
(38) Tsang, W. In *Shock Waves in Chemistry*; Lifshitz, A., Ed.; Marcel Decker: New York, 1981; pp. 59–129.
(39) Awan, I. A.; Burgess Jr, D. R.; Tsang, W.; Manion, J. A. Standard reactions for comparative rate studies: Experiments on the dehydrochlorination reactions of 2-chloropropane, chlorocyclopentane, and chlorocyclohexane. *Int. J. Chem. Kinet.* **2012,** *44,* 351-368.
(40) Goodwin, D. G.; Moffat, H. K.; Speth, R. L. *Cantera: An object- oriented software toolkit for chemical kinetics, thermodynamics, and transport processes*, Version 2.3.0. **2017**.
(41) Sheen, D. A.; Rosado-Reyes, C. M.; Tsang, W. Kinetics of H atom attack on unsaturated hydrocarbons using spectral uncertainty propagation and minimization techniques. *Proc. Combust. Inst.* **2013,** *34,* 527-536.
(42) Tsang, W.; Walker, J. A. Mechanism and rate constants for the reactions of hydrogen atoms with isobutene at high temperatures. *Symp. (Int.) Combust.* **1989,** *22,* 1015-1022.
(43) Blitz, M. A.; Green, N. J. B.; Shannon, R. J.; Pilling, M. J.; Seakins, P. W.; Western, C. M.; Robertson, S. H. Reanalysis of rate data for the reaction $CH_3 + CH_3 \rightarrow C_2H_6$ using revised cross sections and a linearized second-order master equation. *J. Phys. Chem. A* **2015,** *119,* 7668-7682.

(44) Tokmakov, I. V.; Lin, M. C. Combined quantum chemical/RRKM-ME computational study of the phenyl + ethylene, vinyl + benzene, and H + styrene reactions. *J. Phys. Chem. A* **2004,** *108,* 9697-9714.
(45) Tsang, W. Chemical kinetic data-base for combustion chemistry. 3. propane. *J. Phys. Chem. Ref. Data* **1988,** *17,* 887-952.
(46) Tsang, W. Chemical kinetic data base for combustion chemistry 4. isobutane. *J. Phys. Chem. Ref. Data* **1990,** *19,* 1-68.
(47) Baulch, D. L.; Cobos, C. J.; Cox, R. A.; Frank, P.; Hayman, G.; Just, T.; Kerr, J. A.; Murrells, T.; Pilling, M. J.; Troe, J., et al. Evaluated kinetic data for combustion modeling. supplement I. *J. Phys. Chem. Ref. Data* **1994,** *23,* 847-848.
(48) Brand, U.; Hippler, H.; Lindemann, L.; Troe, J. Carbon-carbon and carbon-hydrogen bond splits of laser-excited aromatic molecules. 1. Specific and thermally averaged rate constants. *J. Phys. Chem.* **1990,** *94,* 6305-6316.
(49) Sheen, D. A.; Wang, H. The method of uncertainty quantification and minimization using polynomial chaos expansions. *Combust. Flame* **2011,** *158,* 2358-2374.
(50) Wang, H.; Sheen, D. A. Combustion kinetic model uncertainty quantification, propagation and minimization. *Prog. Energy Combust. Sci.* **2015,** *47,* 1-31.
(51) Sheen, D. A.; Manion, J. A. Kinetics of the reactions of H and CH_3 radicals with *n*-butane: An experimental design study using reaction network analysis. *J. Phys. Chem. A* **2014,** *118,* 4929-4941.
(52) Sheen, D. A. *Method of Uncertainty Minimization using Polynomial Chaos Expansions*; National Institute of Standards and Technology: Gaithersburg, MD, **2017**.
(53) Robaugh, D.; Tsang, W. Mechanism and rate of hydrogen atom attack on toluene at high temperatures. *J. Phys. Chem.* **1986,** *90,* 4159-4163.
(54) Walker, J. A.; Tsang, W. Single-pulse shock-tube studies on the thermal-decomposition of normal-butyl phenyl ether, normal-pentylbenzene, and phenotole and the heat of formation of phenoxy and benzyl radicals. *J. Phys. Chem.* **1990,** *94,* 3324-3327.
(55) Baldwin, R. R.; Keen, A.; Walker, R. W. Rate constants for the addition of methyl radicals to propene. *J. Chem. Soc., Faraday Trans. 2* **1987,** *83,* 759-766.
(56) Metcalfe, E. L.; Trotman-Dickenson, A. F. The reactions of alkyl radicals. Part VIII. Isobutyl radicals from the photolysis of isovaleraldehyde. *J. Chem. Soc.* **1960,** *0,* 5072-5078.
(57) Ratkiewicz, A. Kinetics of the C-C bond beta scission reactions in alkyl radicals. *Phys. Chem. Chem. Phys.* **2011,** *13,* 15037-15046.
(58) Goos, E; Burcat, A; Ruscic, B. Extended Third Millennium Ideal Gas and Condensed Phase Thermochemical Database for Combustion with Updates from Active Thermochemical Tables. received from Elke Goos, Elke.Goos@dlr.de, 15. August 2017.
(59) Tsang, W.; Cui, J. P.; Walker, J. A. Single pulse shock tube studies on the reactions of hydrogen atoms with unsaturated compounds. *AIP Conf. Proc.* **1990,** *208,* 63-73.
(60) Manion, J. A.; Louw, R. Rates and mechanisms of gas-phase desubstitution of hexadeuteriobenzene and benzene-derivatives $C_6H_5CH_3$, $C_6H_5CF_3$, C_6H_5OH, C_6H_5Cl, and C_6H_5F by H-atoms between 898-K and 1039-K. *J. Phys. Chem.* **1990,** *94,* 4127-4134.

(61) Ellis, C.; Scott, M. S.; Walker, R. W. Addition of toluene and ethylbenzene to mixtures of H_2 and O_2 at 772 K: Part 2: Formation of products and determination of kinetic data for H+ additive and for other elementary reactions involved. *Combust. Flame* **2003,** *132,* 291-304.
(62) Oehlschlaeger, M. A.; Davidson, D. F.; Hanson, R. K. Experimental investigation of toluene + H → benzyl + H_2 at high temperatures. *J. Phys. Chem. A* **2006,** *110,* 9867-9873.
(63) Müller-Markgraf, W.; Troe, J. Shock wave study of benzyl UV absorption spectra: Revised toluene and benzyl decomposition rates. *Symp. (Int.) Combust.* **1988,** *21,* 815-824.
(64) Lefort, B.; Tsang, W. High temperature stability of larger aromatic compounds. *Combust. Flame* **2011,** *158,* 657-665.
(65) Hippler, H.; Reihs, C.; Troe, J. Elementary steps in the pyrolysis of toluene and benzyl radicals. *Zeitschrift Fur Physikalische Chemie Neue Folge* **1990,** *167,* 1-16.
(66) Gardiner, W. C.; Troe, J. In *Combustion Chemistry*; Gardiner, W. C., Ed.; Springer-Verlag: New York, 1984; pp 173-196.
(67) Barker, J. R.; Ortiz, N. F. Multiple-well, multiple-path unimolecular reaction systems. II. 2-methylhexyl free radicals. *Int. J. Chem. Kinet.* **2001,** *33,* 246-261.
(68) Mertens, L.A.; Awan, I.; Manion, J.A. **2018.** In Preparation.
(69) Marsi, I.; Viskolcz, B.; Seres, L. Application of the group additivity method to alkyl radicals: an *ab initio* study. *J. Phys. Chem. A* **2000,** *104,* 4497-4504.
(70) Benson, S.W. *Thermochemical Kinetics,* 2nd ed.; Wiley: New York, 1976.
(71) Lay, T. H.; Bozzelli, J. W.; Dean, A. M.; Ritter, E. R. Hydrogen atom bond increments for calculation of thermodynamic properties of hydrocarbon radical species. *J. Phys. Chem.* **1995,** *99,* 14514-14527.
(72) Gurvich, L. V.; Veyts, I. V.; Alcock, C. B. *Thermodynamic Properties of Individual Substances*. 4th ed.; Hemisphere: New York, 1991.
(73) Viskolcz, B.; Lendvay, G.; Seres, L. Ab initio barrier heights and branching ratios of isomerization reactions of a branched alkyl radical. *J. Phys. Chem. A* **1997,** *101,* 7119-7127.
(74) Benson, S. W.; Buss, J. H. Additivity rules for the estimation of molecular properties. Thermodynamic properties. *J. Chem. Phys.* **1958,** *29,* 546-572.
(75) Afeefy, H. Y.; Liebman, J. F.; Stein, S. E. NIST Organic Thermochemistry Archive (NOTA). In *NIST Chemistry WebBook*; Linstrom, P. J.; Mallard, W. G., Eds.; NIST Standard Reference Database Number 69; National Institute of Standards and Technology: Gaithersburg MD, http://webbook.nist.gov, (retrieved March 27, 2018)
(76) Poutsma, M. L. Evaluation of the kinetic data for intramolecular 1,x-hydrogen shifts in alkyl radicals and structure/reactivity predictions from the carbocyclic model for the transition state. *J. Org. Chem.* **2007,** *72,* 150-161.
(77) Davis, A. C.; Francisco, J. S. Ab initio study of hydrogen migration across n-alkyl radicals. *J. Phys. Chem. A* **2011,** *115,* 2966-2977.
(78) Konar, R. S.; Marshall, R. M.; Purnell, J. H. Initiation of isobutane pyrolysis. *Trans. Faraday Soc.* **1968,** *64,* 405-413.
(79) Stepukhovich, A. D.; Babayan, V. I. Intramolecular rearrangements of hydrocarbon radicals in the gas-phase. *Russ. Chem. Rev.* **1972,** *41,* 750-758.
(80) Manion, J. A.; Awan, I. A. The decomposition of 2-pentyl and 3-pentyl radicals. *Proc. Combust. Inst.* **2013,** *34,* 537-545.

(81) Robertson, S. H.; Pilling, M. J.; Jitariu, L. C.; Hillier, I. H. Master equation methods for multiple well systems: Application to the 1-,2-pentyl system. *Phys. Chem. Chem. Phys.* **2007,** *9,* 4085-4097.
(82) Ratkiewicz, A.; Truong, T. N. Kinetics of the C–C bond beta scission reactions in alkyl radical reaction class. *J. Phys. Chem. A* **2012,** *116,* 6643-6654.

TOC Graphic

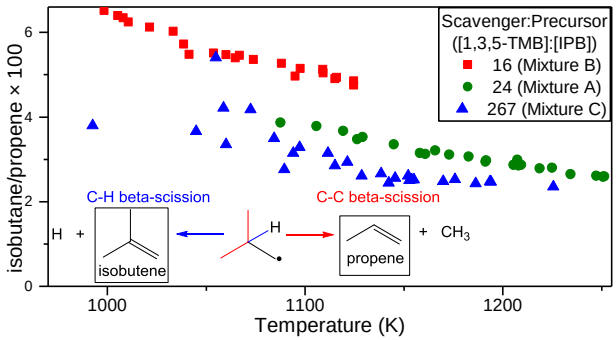
Scavenger:Precursor
([1,3,5-TMB]:[IPB])
16 (Mixture B)
24 (Mixture A)
267 (Mixture C)
isobutane/propene × 100
Temperature (K)
C-H beta-scission
C-C beta-scission
H +
isobutene
H
propene
+ CH3